UNIVERSITY of RWANDA COLLEGE OF SCIENCE AND TECHNOLOGY ACE-ESD AFRICAN CENTER OF EXCELLENCE IN ENERGY FOR SUSTAINABLE DEVELOPMENT

Dissertation Title:

"DESIGN OF FLOATING SOLAR PHOTOVOLTAIC SYSTEM INTEGRATED WITH A HYDROPOWER PLANT (A CASE STUDY NYABARONGO HPP DAM)"

By

SAMVURA Jean de Dieu

Reference Number : 220004580

A dissertation submitted to the African Center of Excellence in Energy Studies for Sustainable Development (ACE-ESD)

College of Science and Technology, University of Rwanda

In Partial Fulfillment of the Requirement for the Degree of Masters of Science

in

ELECTRICAL POWER SYSTEMS

PROJECT ID: ACEESD/EPS/21/17

Supervisor: Dr. JMV BIKORIMANA

Co-Supervisor: Mr. Aphrodis NDUWAMUNGU

November, 2021 **Kigali-Rwanda**

DECLARATION

I, the undersigned, declare that this Project entitled **''Design of FSPV system integrated with a hydropower plant (A case study NYABARONGO HPP Dam)''**is my original work, and has not been presented for a degree in University of Rwanda or any other universities. All sources of materials that were used for the dissertation work were acknowledged.

Name : Mr. SAMVURA Jean de Dieu Signature : 

CERTIFICATION

This is to certify that the dissertation work titled "Design of FSPV system integrated with a hydropower plant (A case study NYABARONGO HPP Dam)" submitted by Mr. SAMVURA Jean de Dieu is an authentic dissertation work completed under my supervision and assistance and meeting the nature and standard required for the partial fulfillment of the Degree of Masters of Science in Electrical Power Systems. The work contained in this dissertation has not been submitted for a Degree elsewhere.

Date of Submission: 3rd November, 2021

Dissertation Supervisor: Dr. JMV BIKORIMANA Signature

ACKNOWLEDGEMENTS

This research thesis would not have been possible without the guidance and assistance of several individuals who contributed and extended their valuable assistance in various ways during the study's preparation and completion. First and foremost, I thank God for his never-ending love, mercy, and gift of life.

Working as Msc. scholar at the University of Rwanda was both a wonderful and challenging experience for me. Completing the research and writing the thesis is more difficult and rewarding than I could have imagined. I am grateful to the African Center of Excellence in Energy Studies for Sustainable Development (ACE-ESD) for providing me with the opportunity to pursue a Master of Science degree in Electrical Power Systems at the University of Rwanda/College of Science and Technology (CST).

I would like to express my heartfelt appreciation to Rwanda Polytechnics and IPRC-Musanze for allowing me to continue my studies and earn this Master's degree.

I owe Dr. JMV BIKORIMANA an enormous debt of gratitude for his invaluable advice, brilliant ideas, efficacy, humility, continuous availability, assistance, guidance, support, and instructive comments, all of which contributed to the smooth success of this work. He generously gave of his time to discuss the concept and offer suggestions for improvement. This work would not have been completed without his invaluable assistance and valuable experience. I will never pass up an opportunity to make him proud.

The best lecturers I have ever had, who gave me the confidence to dream big. Thank you for giving me confidence. Your optimism and kindness made me feel so at ease. Your inspiration made me a more thoughtful person, and your encouragement made my days brighter.

I would like to thank my wife IMANISHIMWE Angélique for her love, care, support, and sound advice.

Finally, my heartfelt gratitude goes to my family, relatives, and friends, as well as everyone else who contributed directly or indirectly to the completion of this project; your advice and support were extremely valuable to me during this studying journey.

ABSTRACT

Renewable energy, particularly solar photovoltaic, offers great solutions to the current energy crisis that people face in their daily lives due to its cleanliness, advantages, and low cost of technology. The dissertation intends to demonstrate to the public, policymakers, and policy executors that sufficient exploitation of available water resources and solar energy abundant in the country can ensure the sustainability of electric energy as well as renewable energy development in Rwanda. The dissertation's main goal is to design a floating solar photovoltaic system integrated with a hydropower plant (a case study of the NYABARONGO Dam). The potential energy of floating solar photovoltaic (FSPV) on the Nyabarongo hydro power plant (HPP) dam is modeled and simulated using PVsyst software, and Matlab was used to validate the thesis results and analyze the impact of floating solar photovoltaic (FSPV) integrated with hydropower plant on the national grid. The control system includes a maximum power point tracker, which locates the point at which the photovoltaic modules produce the most power under varying operating conditions. The phase locked loop (PLL) is used to quickly synchronize the PV system with the grid by locking the converter output to the grid voltage. The rotating reference frame locked to the grid is used to control current and voltage towards active and reactive power flow. Furthermore, the study demonstrates the benefits and potential of using floating solar photovoltaic (FSPV) in Rwanda to reduce the use of land-mounted solar photovoltaic (SPV), as floating solar photovoltaic (FSPV) is found to be more efficient than traditional SPV due to its cooling facilities. A total of 33,750 photovoltaic modules were used on a small surface area of 72,884 m^2 extracted from a large surface area of the Nyabarongo hydro power plant (HPP) dam, injecting 15 MWp into the grid at a nominal power ratio of 1. Five 3,000 kW inverters, each operating at 630-930 V_{DC} and 400 V_{AC} at its output, were used to connect the FSPV to the grid, and MATLAB software (Version 2017) was used to simulate its performance with an inductor-capacitor-inductor (LCL) filter. The proposed model includes PV arrays, a closed loop boost converter to control the effects of weather on the floating solar photovoltaic (FSPV), and an inverter with an LCL filter to suppress harmonics in the system. The system parameters were tuned so that the total harmonics distortion of current and voltage respects the IEEE (519-2014) standards. It is ensured that the production of Nyabarongo hydro power plant (HPP) has been improved because with FSPV inject 28 MW or more into the grid at all times. The results show that the floating solar photovoltaic (FSPV) makes the best use of existing infrastructure and could supplement existing hydroelectric production as well as provide electricity in conjunction with hydro power plant's existing generating units.

TABLE OF CONTENTS

LIST OF FIGURES

LIST OF TABLES

ABREVIATIONS AND ACRONYMS

AC	Alternating Current
AI	Artificial Intelligent
ANN	Artificial Neural Network
A_{PV}	Total panel area
BIPV	Building Integrated Photovoltaic
C_b	Boost Capacitance
C_f	Filter Capacitance
CO2	Carbone Dioxide
C_{TI}	Temperature coefficient of current
C_{TV}	Temperature coefficient of voltage
DC	Direct Current
EPO	Electric Power Output
ESMAP	Energy Sector Management Assistance Program
FF	Fill Factor
FFT	Fast Fourier Transform
FOCV	Fractional Open Circuit Voltage
FSCC	Fractional Short-Circuit Current
FSPV	Floating Solar Photovoltaic
GA	Genetic Algorithm
GHGS	Green House Gases
GW	Giga Watt
GWh	Giga Wat-hour
GWp	Giga Watt peak
HPP	Hydo Power Plant
IC	Incremental Conductance
IEEE	Institute of Electrical and Electronics Engineering
KVA	Kilo-Volt-Ampere
KW	Kilo-Watt
L_b	Boost Inductance

L_f	Filter Inductance
MININFRA	Ministry of Infrastructure
MVA	Mega-Volt-Ampere
MW	Mega Watt
MWp	Mega-Watt peak
NASA	National Aeronautics and Space Administration
P&O	Perturbation& Observation
PMSPV	Pole mounted solar photovoltaic
P_{PV}	Photovoltaic power
PR	Performance Ratio
PSO	Particle Swarm Optimization
PV	Photovoltaic
RCC	Ripple Correlation Control
REG	Rwanda Energy Group
RES	Renewable Energy Resources
R_f	Filter damping Resistor
RMS	Root Means Square
SERIS	Solar Energy Research Institute of Singapore
SPV	Solar Photovoltaic
STC	Standard Test Conditions
TERI	The Energy and Resource Institute
THD	Total Harmonics Distortion
T_W	Sea Water Temperature
TWh	Tera-Watt-hour
T_{WS}	The Sea wind Speed
Z_b	Base Impedance

CHAPTER I: INTRODUCTION

1.0. Background

Rwanda currently has a total installed power generation capacity of 235.6 MW, with an estimated 51 percent of the population having access to electricity (37 on-grid and 14 percent off-grid). Rwanda aims to reduce the use of biomass (wood energy) from 79.9 percent to 42 percent by 2024, increase access to electricity to 100 percent by 2024 (52 percent on grid and 48 percent off-grid), and productive users to be connected 100 percent by 2022, as well as achieve 556 MW installed power generation capacity by 2024.

In 2017, Rwanda distributed more than 185,000 solar home systems and nearly 300,000 solar lanterns. This activity is on track to meet Rwanda's target of off-grid electrification of 48 percent by 2024, as shown in [1]. As shown in Fig.1.1, the growth of power generation from 2010 to 2013 is small and nonlinear, whereas the growth of power generation from 2013 to 2021 is significant and approximated to be linear. The plot of Fig.1.1 (a) depicts installed capacity growth per year from 2010 to 2021. The graph shows a significant increase from 2013 to the present.

1.1. Rwanda's population growth rate in relation to land

Rwanda's population growth rate is high in comparison to land resources [2], so land resources used for solar energy generation must be reduced and replaced with another alternative of energy generation that does not use land.

Rwanda distributed over 185,000 solar home systems and nearly 300,000 solar lanterns in 2017. This activity is on track to meet Rwanda's target of 48 percent off-grid electrification by 2024, as shown in Fig.1.1 (b). This scenario leads to increased water, food, and energy consumption in Rwanda, putting pressure on land, biomass resources, and water ecosystems as a result of the country's high population, negatively affecting the climate.

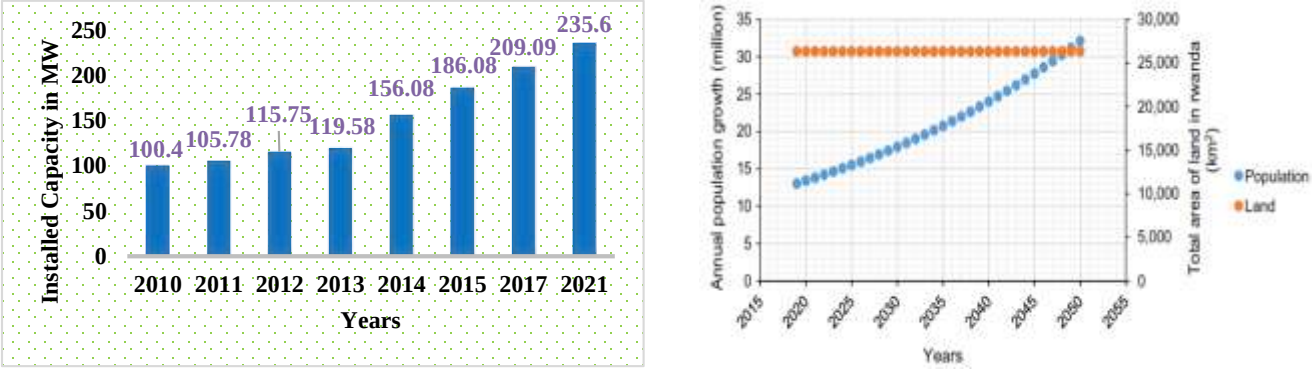

(a) (b)

Figure1. 1: Installed capacity and population growth (a) Increase in installed capacity in MW per year (source REG Website, and (b) Annual Population projection against available land in Rwanda, 2019-2050 [2]

It has been demonstrated that traditional terrestrial PV systems produce only 1 kW for a large land surface of 8 m^2, posing enormous challenges in terms of land resource. Based on the foregoing, another alternative in PV energy generation technology may offer a synthetic solution for energy production that does not place a significant demand on land resources. A floating PV system is a new type of solar energy generation technology in which PV cells are installed on a floating system on the surface of the water. In 2007, the first study on floating PV cells was conducted to compare the performance of floating PV cells with traditional terrestrial PV systems[2]. The research revealed that the FSPV is profitable due to its high efficiency.

1.2. Statement of the problem

Rwanda has been trying to overcome the challenge of energy production. It is in this prospective that the government has started to exploit the energy from Solar photovoltaic (PV). Fig.1.3 shows Rwamagana SPV power plant as a typical example [1]. This solar power plant takes up the entire 17 hectares (170,000 square meters) of land, employs 28,360 photovoltaic panels, and generates 8.5 MWp of grid-connected power, enough to power 15,000 homes. The plant is the second large-scale solar field in East Africa, and it now accounts for approximately 6% of the country's total electrical supply. This proves that if the power produced by terrestrial SPV is increased, the native people may face a land crisis, as Rwanda is a small country with a surface area of 26,338 km^2 and 90 percent reliant on agricultural activities [5].

Figure1. 2: Utility-scale of 8.5 MW PV power plant constructed in Agahozo-Shalom Youth Village [4]

Based on equation (1), the land used for energy generation from solar PV indicates a huge reduction in agriculture land if not replaced with other alternatives. The PV energy produced is proportional to the surface occupied by PV modules as indicated by equation (1):

$$P_{PV} = N_P \times A_{PV} \times G \times \eta_{PV} \quad (1)$$

Where: P_{pv} is solar power plant output and N_P: is the total number of panels, A_P: is the total panels' area, G: is the irradiance at STC (1000 W/m^2), andη_{PV}: is the global efficiency of panels.

Referring to existing Rwamagana GigaWatt solar power plant Fig.1.2 occupying the 17 Ha for 8.5 MWp maximum expected output power. If this power is doubled, the required land is about 34 Ha which is a large land surface that can satisfy a big number of population, when it is used for agricultural activities

1.3. Objectives

The thesis has two types of objectives: Major objective and specific objectives. The major objective is the general goal of the present work whereas the specific objectives reflect some activities, which have been conducted toward the major objective.

1.3.1. Major Objective

The primary goal of this dissertation is to design a floating solar PV system on the dam of the NYABARONGO hydropower plant. This floating solar PV (FSPV) system's primary goal is to support the existing hydropower plant (HPP) if energy production from the HPP is reduced or if energy demand increases. The FSPV on the HPP dam can use existing energy transmission resources, allowing for greater flexibility in power dispatch to the grid.

1.3.2. The Specific Objectives

To achieve the main objective, the dissertation has the following specific objectives:

- ✓ Select appropriate solar modules, and inverter depending on meteorological and geographical data of the site.
- ✓ Modeling of the system to show its technical feasibility.
- ✓ Simulate and analyze the performance of the modelled system by MATLAB
- ✓ Analysis of energy potential of FSPV, and solar panels shading effect by PVsyst software
- ✓ Show to the public that FSPV is feasible in Rwanda
- ✓ Show to the policy maker that FSPV contribute to land use management
- ✓ Show to the public that FSPV efficiency is improved compared to traditional SPV efficiency.

1.4. Scope of the study

Based on the limited time, this research dissertation has been focusing on floating photovoltaic system at Nyabarongo HPP dam. The activity to be conducted is to model and simulate the floating system on extracted area.

1.5. Expected Outcomes and Significance of the Study

In this research the expected outcomes part includes all activities expecting to conduct for available time of the research leading to its implication to mitigate existing gaps in energy generation sustainability.

1.5.1. Expected Outcome of the Study

Expected outcome of the designed floating PV system are:

- Prove to Energy developers and policy makers that FSPV is feasible in Rwanda
- Demonstrate that FSPV is one of the key solution to land use management
- FSPV can be used for evaporation minimization for different HPP dams
- Contribute to Rwanda electrification program through scientific research

- Inject the produced power to NYABARONGO HPP bus
- Compensate the peak load demand during a single generator operation
- Lower the GHGS emission to meet the target of Rwanda for its sustainable energy sector
- Lower the dependency of fossil fuel energy
- Lower conventional Solar PV plant use
- Maximize utilization of existing infrastructures.
- Increases the capacity factor of current hydro power plant

1.5.2. Significance of the Study

Because of dam water evaporation in arid areas, global hydroelectric energy fluctuates. The floating PV system protects the dam surface from direct solar radiation, which can have a negative impact on the dam's stability, reduces thermal excursion of the dam surface and increases dam durability, oxygenates water bodies, and reduces land use for hydropower plants. Furthermore, FSPV can be connected to the grid to meet rising load demand. Because of its superiority over land-based solar PV, floating solar PV coupled with hydropower plants have recently grown in popularity around the world[3]. First, floating solar PV systems installed on dams transmit generated power via the existing grid. Second, because relatively cold water cools the PV panels, floating PV systems produce more electric power output (EPO) than land-based PV systems. Third, because floating PV arrays are installed on water, national land can be managed well and used for agricultural purposes, allowing it to be used to its full potential. Fourth, unlike most PV systems installed on land, floating PV systems are less obtrusive because they are not generally visible to the general public. Fifth, structures built on bodies of water are subject to fewer rules and regulations. Fifth, this method aids in the control of algae and the creation of fish-spawning habitats.

1.7. Organization of the study

This research comprises four chapters:

Chapter 1: Introduction, this chapter mainly deals with the rational, and objectives of the study, and ends up the dissertation outlines.

Chapter 2: Solar PV mounting technologies, this chapter is dedicated to illustrate the relevant literatures on land mounted solar PV, in building solar PV, Floating solar PV, the shadow effect on each mounting technology and the way forward to mitigate the shading effect on the solar PV system performance.

Cha**pter 3: Floating PV system development methodology**, the documentation, site data collection, and modeling and simulation as activities conducted in the research are detailed in this chapter.

Chapter 4: Floating PV system modelling and simulation, in this chapter, modeling, and simulation of floating PV are described in details.

Chapter 5: Conclusions and recommendations, is the last part concerned with conclusions, and recommendations of the study. The detail result sheets, photographs etc. are presented in appendix afterwards.

CHAPTER II: SOLAR PV SYSTEM MOUNTING TECHNOLOGIES

2.0. Introduction

Due to its geographical location, solar energy is the most promising renewable energy resource in Rwanda. Rwanda is located south of the equator at 2° 0′ 0″ South and 30° 0′ 0″ East, making it a good candidate for solar energy, with an average daily global solar irradiation on the tilted surface of around 5.2 kWh/m^2 per day[4].

Solar energy is a zero-emission, low-cost, and environmentally friendly energy source. Every day, the sun emits massive amounts of energy in the form of heat and light. PV systems almost all have the same functionality, but they are mounted in different ways. There are numerous PV mounting technologies available; however, in this study, land mounted, building integrated, rooftop mounted, and floating solar PV mounting are discussed. The point to consider during the construction of each solar PV mounting technology is the shadow effect. In [5], when it comes to mounting solar modules, solar energy users have several options. When deciding on the best mounting method, consider the available space, system size, array tilt, orientation, shading, durability, and cost. Based on the aforementioned factors, researchers are working hard to improve wind speed loading, snow load, tilt angle, and site geography for each mounting technology in order to improve solar module performance.

2.1. Solar PV mounting technologies

Mounting of solar module is the one technical point considered when determining; wind loading size, snow loading, tilt angle, shading effect on the PV module, and tracking direction of the solar module. In nature, most mounting solar PV systems are fixed-plate in design. When a solar photovoltaic PV system is installed to provide an unobstructed view of the sun, it is possible to use the sun to generate electricity for residential, commercial, or agricultural purposes. Installing a single solar module or a solar array at the proper tilt angle is part of this. When it comes to mounting solar modules, the solar user has several options. When deciding on the best mounting method, consider the available space, system size, array tilt, orientation, shading, durability, and cost[5].The solar PV power plant mounting is broadly divided into various types such as roof mounted, ground mounted, pole mounted, ballast mounted, flush mounted, floating solar PV, building mounted solar PV, and East-West mounted solar PV as indicated in Fig.2.1.

(a) Roof mounted SPV at I & M Bank/Rwanda

(b) Ground mounted SPV at Rwamagana

(c) PMSPV Sahasra Electronics Rwanda

(d) Ballast mounted solar PV

(e) Flush mounted solar PV

(f) Floating solar PV

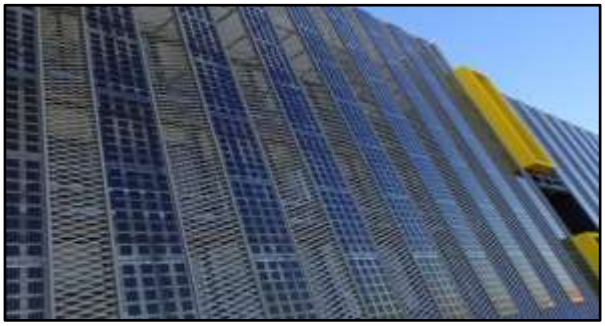

(g) Build-integrated solar PV

(h) East-west mounting of solar modules

Figure2. 1:Examples of different types of solar PV mounting: (a) Roof mounted solar PV, (b) Ground mounted solar PV, (c) Pole mounted solar PV, (d) Ballast mounted solar PV, (e) Flush mounted solar PV, (f) Floating solar PV, (g) Build-integrated solar PV, and (h)East-West mounting of solar modules [6],[7], [8],[9], [10]

2.1.1. Land mounted solar PV

Traditional solar PV is a land-based or ground-mounted solar PV system. A ground mounted solar system works well in areas where there is enough space to install the system away from buildings and shade producing structures. It is more expensive than roof-mounted solar PV. Modules are mounted on rails that are attached to concrete pylons or blocks or fixed to a steel structure installed in the ground. Installation, maintenance, cooling, and safety are all simple with this type of mounting. Figure 2.1(b) depicts ground-mounted solar PV. The available irradiance and ambient temperature dictate the output power and generation efficiency of ground-mounted solar PV systems, as detailed in [11]. For land mounted PV system output power and its generation efficiency are respectively determined by equation (2), and (3).

$$P_{PV} = A_{PV} \times G_T \times \eta_{PV} \quad (2)$$

$$\eta_{PV} = \eta_r \times \eta_{PC}[1 + \alpha_p(T_C - T_{C,STC})] \quad (3)$$

Where: A_{PV} is the PV module area, GT is the solar irradiance on the plane of PV arrays, η_{PV} is the PV generation efficiency, and η_{PV} and η_r are the power conditioning and reference module efficiencies, respectively. STC denotes the PV cell temperature under standard test conditions (STC), TC denotes the PV cell temperature, and α_P denotes the temperature coefficient of power.

2.1.2. Building integrated solar PV

PV cells can be mounted on top of or above existing or traditional roofing or wall systems, as shown in Fig2.1 (g). BIPV (Building integrated solar PV) can function as both a climate control device and a power source that generates electricity. Thus, in addition to lowering electricity costs, BIPV may provide material and labor savings. Furthermore, major factors to consider and assess when integrating PV cells into the outer building envelope skin include cell aeration, cell inclination, coverage area, cell geographical position, and orientation towards the sun[8]. The shading effect consideration for this technology is a must. Evaluation of BIPV is based on the important technical characteristics indicated in equations (4) and (5)

$$\eta = P_{max}/(\Phi\, A) \quad (4)$$

$$FF = P_{max}/U_{oc}I_{sc} = U_{max}I_{max}/U_{oc}I_{sc} \quad (5)$$

Where P_{max} is the maximum power point in watt-peak (Wp), Φ is the input solar irradiance in W/m^2, FF is a fill factor, U_{OC} is the open-circuit voltage in Volts, and I_{Sc} is the short-circuit current in Amps.

Researchers' efforts in developing PV and BIPV materials and technologies will result in increasingly better BIPV solutions in the coming years, owing to improved solar cell efficiency, environmental aspects, lower production costs, and improved building integration.

2.1.3. Floating solar PV

The floating photovoltaic system (FPVS) is a novel approach to renewable energy production that does not add to the strain on water and land resources. As shown in the diagram of Fig.2.1 (f), FSPV, also known as floatovoltaics, is a solar PV application in which PV panels are designed and installed to float on bodies of water such as reservoirs, hydroelectric dams, industrial ponds, irrigation ponds, water treatment ponds, mining ponds, wastewater treatment plants, wineries, fish farms, canals, lakes, oceans, and lagoons. This mounting technology offers more advantages over traditional land mounted solar system due to its cooling done by water and air circulating on water surface. Key components of a large scale FSPV is shown in Fig.2.2.

The integration of FSPV with existing hydropower plant increase its capacity factor as well its performance towards its reliability[12]. Moreover, in [13], the researcher showed that if the HPP dam surface is covered with FSPV module to 10% , HPP energy production has been increased by 65%. The main factors that determine cell temperature in a floating PV system are wind speed and sea temperature[14].

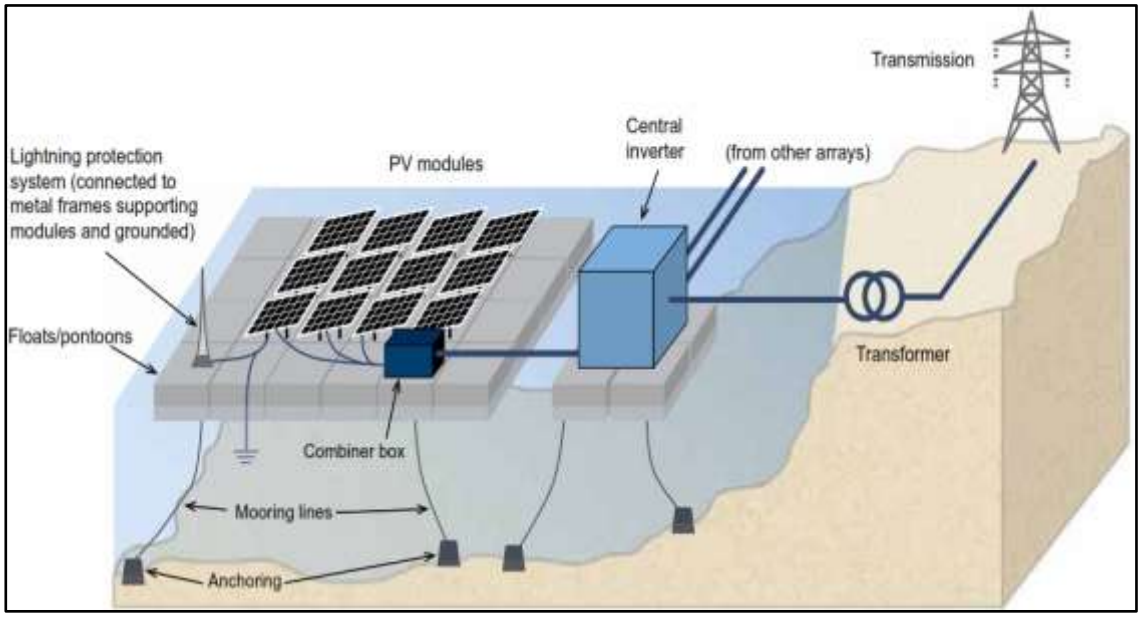

Figure2. 2: A schematic depiction of a typical large-scale FSPV system and its key components [15]

Water temperature, wind velocity, and floating PV array output can be determined using equations (6), and (7).

$$T_W = 5 + 0.75T_{amb} \quad (6)$$

$$V_{ws} = 1.62 + 1.17V_{wl} \quad (7)$$

Where, T_W is the sea temperature, T_{amb} is the air temperature in (^oC), V_{ws} is the sea wind speed, and V_{wl} is the land wind speed in m/s, respectively. The cell temperature on the sea is given by equation (8)

$$T_{cw} = 0.943T_w + 0.0195G - 1.528V_{ws} + 0.3529 \quad (8)$$

Where, T_{cw} is the sea cell temperature.

The floating solar PV array output power can be determined using equation (9)

$$P_{PV\ array} = \frac{E_L}{(\frac{G}{G_{STC}}) \times (f_{DC/AC}) \times f_{temp}} \quad (9)$$

Where, E_L is the estimated energy required per day (Wh/day), $f_{DC/AC}$ is DC to AC de-rating factor [%] = 0.778. Cell temperature is given by equation (10)

$$f_{temp} = 1 - \beta(T_{cw} - T_{STC}) \quad (10)$$

Where, β is the PV cell temperature in current time step (^oC) =-0.38%

The expression in the equation (11) can be used to calculate a photovoltaic module's efficiency or power conversion.

$$\eta_{El} = \frac{P_{max}}{G \times A_{PV}} \times 100\% \quad (11)$$

Where η_{El} is the electricity efficiency produced (%), P_{max} is the maximum power produced by PV system (W), G is the solar radiation strength falling on the PV module (W/m^2), and A_{PV} the area of PV module receiving the irradiance (m^2).

2.1.4. Hybrid FPV-Hydropower systems

A hybrid energy system is preferred for harnessing energy from multiple sources at the same time and location, including both renewable and conventional power plants. In [16], FSPV systems in hybrid systems are identical to those in standalone systems. However, they are coupled with other generation, the author defined hybrid systems as those in which net economic benefits from the coupling of multiple generation technologies are anticipated, relative to the cost and/or value attached with comparable independent, stand-alone technologies, three possible hybridization configurations are suggested in the same research.

1. **Hybrid systems that co-exist (cost savings):** two or more technologies are co-located to save money, but operations are improved separately.
2. **Computer generated hybrid systems (improved performance):** more than two technologies are sited separately, with operations linked via joint agreement and some co-optimized operation.
3. **Fully hybrid systems (cost and performance improvements):** Co-optimized planning and operation achieves both cost and performance improvements. These frequently include at least one dispatchable technology paired with one or more variable renewable technologies that, when combined, provide operational benefits.

The FSPV hybrid technologies include: FSPV-Hydro systems, FSPV-Pumped hydro, FSPV-Wave energy converter, FSPV-Solar tree, FSPV-Tracking, FSPV-Conventional power, and FSPV-Hydrogen as detailed in [17].Among all these highlighted hybrid technologies, FSPV-Hydro system is among the most promising methods that could be potentially used for efficient power generation, it is shown in the previous Fig.2.3.

2.2. Floating solar PV worldwide overview

One option that has gained traction globally and is expected to grow rapidly in the coming years is floating solar PV (FSPV). Annual capacity addition is expected to rise from 1.314 GWp in 2018 to 4.6 GWp by 2022. China is the largest international market at the moment, followed by Japan and South Korea. Due to the availability of large bodies of water, India, according to the research, is another country with very promising prospects for developing FSPV projects[18].

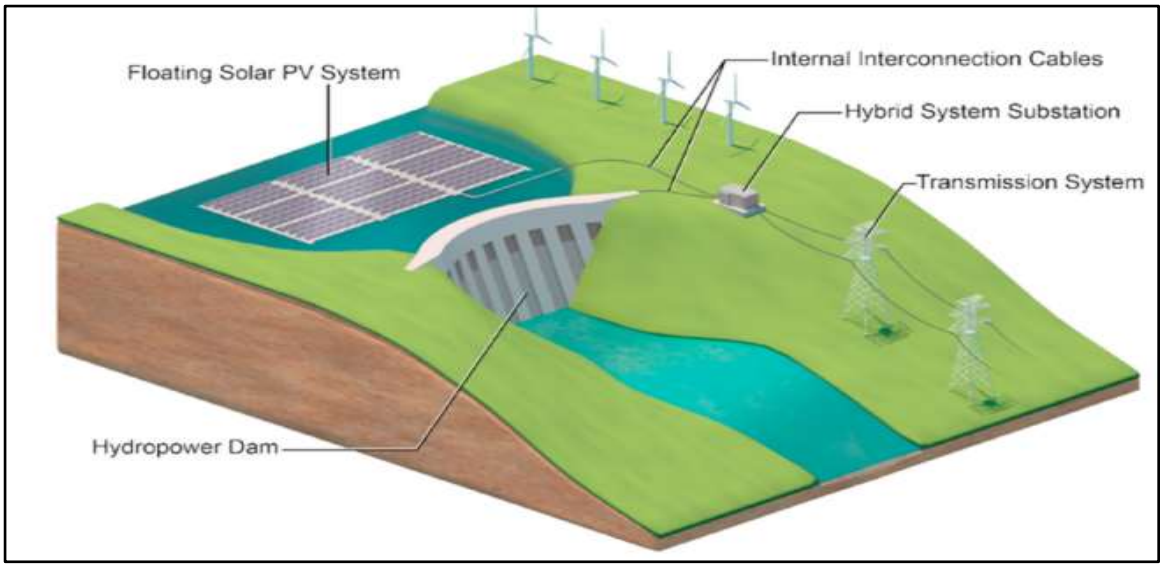

Figure2. 3:Schematic of a hybrid FPV-hydropower system[17]

According to past and current research, if renewable energy generation booms and FSPV installed capacity doubles every year, it is estimated that by 2050, FSPV power plants will produce all of the world's electricity. According to current analysis, this makes sense, as described in [12].

However, the contribution of floating solar PV in renewable energy generation booming, there still one to five data gaps as mentioned in[16]. For starters, there is no global identification on FSPV, and no publicly available bathymetry data sets with the required resolution are available. Due to a lack of bathymetry data, the researchers are unable to estimate water body areas that may be too narrow or have seasonal variations in coverage, preventing FSPV deployment. Second, because there is no global data on the spatial temporal variation of water bodies, it is impossible to exclude areas of water bodies that are dry for a portion of the year. Third, due to system configuration assumptions, global capacity factor data, such as the Global Solar Atlas, is biased toward land-based systems. The Global Solar Atlas data is based on an optimum tilt. As a result, capacity factors for FSPV systems in high latitudes are most likely overestimated. Furthermore, these data do not account for any potential cooling effects of water on FSPV system efficiency, which would increase FSPV capacity factors in warmer climates. These factors could lead to a difference in estimated generation between water bodies in warmer and cooler regions. Fourth, due to a lack of global coverage in hydropower capacity (MW) and annual generation (GWh) per year, it is difficult to size FSPV systems in proportion to hydropower and available transmission system capacities. While this may be a financial concern, the data may also allow for an evaluation of the combined capacities and/or benefits of hybrid FSPV-hydropower systems. Finally, the resolution of attributes at regional scales such as European, country, or sub-country scales remains unchanged for datasets with global coverage.

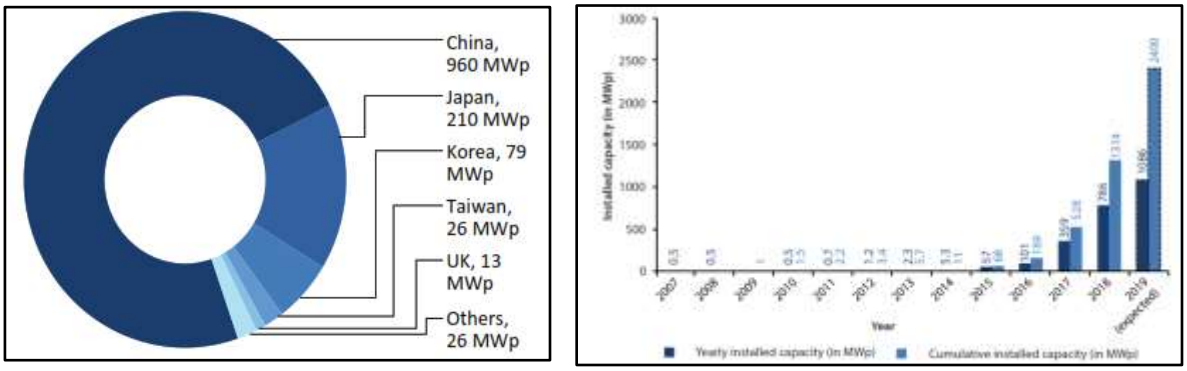

(a) Top 6 countries in the world advancing in FSPV

(b) World FSPV installed capacity in MW_P

Figure2. 4: Global installed SFPV capacity (TERI's analysis based on publicly available sources)[15]

These datasets do not include prospects, local project siting constraints to floating solar PV that reflect water body use regulations (for example, prohibitions on siting on recreational water bodies) or water body conditions (potential freezing during winter months).

In [15], floating solar photovoltaic (FSPV) installations accounted for 1.3 GigaWatt-peak (GWp) of total installed global capacity at the end of 2018, according to the World Bank Group, and deployment is expected to accelerate as the technologies mature, opening up a new frontier in the global expansion of renewable energy. When combined with other demonstrated benefits such as higher energy yield, reduced evaporation, and, in some cases, improved water quality, FSPV is likely to be an appealing option for many countries. To avoid using scarce land resources for solar power generation, several countries with dense populations are considering large-scale floating solar deployment. The author describes China in the same handbook. With the installation of a few large FSPV systems since 2017, it has risen to the top of the market, with more than 950 megawatt-peak (MWp) installed capacity in 2018, accounting for roughly 73 percent of the global total shown in Fig.2.4 (a). The remaining installed capacity was distributed primarily among Japan, the Republic of Korea, Taiwan, China, and the United Kingdom, with the rest of the world accounting for only 2%. FSPV projects, on the other hand, were being developed in over 30 countries (World Bank Group, ESMAP, and SERIS 2019). As shown in Fig.2.4 (b), the total installed capacity of FSPVs worldwide from 2007 to 2019 was 2400 MWp.

The competition between hydroelectric, GSPV, and wind energy sectors is clearly depicted in Fig.2.5 (a), with the SPV dominating after 2027.[12].

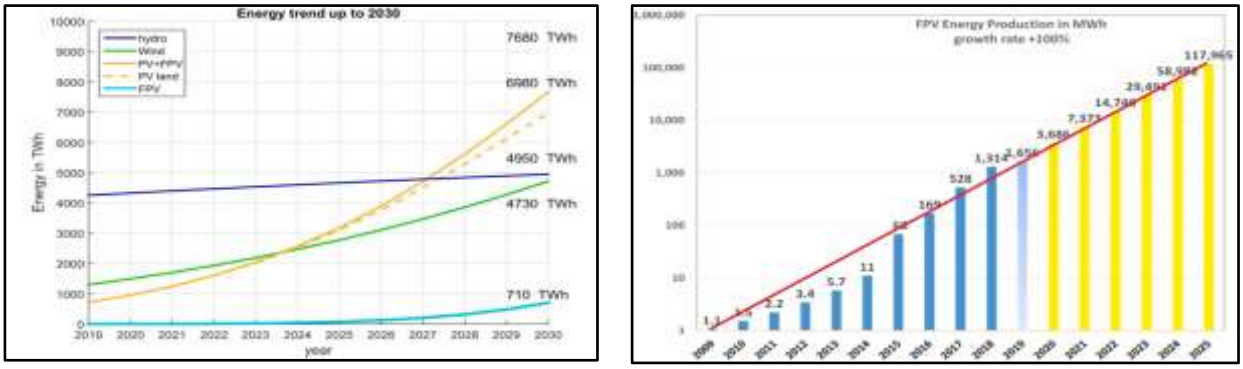

(a) (b)

Figure2. 5:Renewable energy growth trend: (a) Plot of RES growth in the next ten years in linear scale, (b) Logarithmic plot of global yearly produced FPV energy (blue, 2019 to be confirmed) and forecast up to 2025 (yellow). The red line represents a linear fit with a fixed growth rate of 100%. [12]

In this research, the author predicts the renewable energy sources without considering intermittency of solar, wind and environmental impact of this kind of booming of FSPV and wind energy sources use. The trend of hydro, wind, SPV-FSPV, GSPV, FSPV from 2019 to 2030 are respectively, 4,950; 4,730; 6,980; and 710 TWh as indicated in Fig.2.5 (a). The SPV-FSPV combination has higher trend compared to other source of energy.

The logarithmic trend in FSPV energy production in MWh is shown in the Fig.2.5 (b), it is shown that, the FSPV energy production is increasing linearly from 2009 to 2025 (1.1 MWh to 117,965 MWh).

2.3. FSPV internal and external negative impacts

In [19], the researcher presented internal negative impacts of FSPV such as FSPV requires long-term maintenance requirements and the durability of floating solar PV is yet to be seen, ecological and adverse effects on water ecosystem, relatively young and immature technology, lack of experience and knowledge, lack of cooperation from local distribution utility, solar energy concentration levels on floating platform, high waves and salt water potentially damaging the solar panels. Others, on the other hand, demonstrated how to mitigate FSPV's negative effects, thereby making FSPV profitable.

2.3.1. Challenges with floating solar panels

Presently, floating solar photovoltaic (FPV) still comes with challenges that will require further research and learning to expand its installation all over the world[15]. Some of those challenges includes:

- The capital costs of FPV are currently still slightly higher than ground-mounted PV, owing chiefly to the expenses for the floats, mooring and anchoring, and more stringent requirements for electrical components.
- In some reservoirs, anchoring and mooring installation and maintenance for FSPV becomes a challenging issue due to water depth and the terrain of the water body's bed. For this case more complicated solutions are required and additional cost to the project.
- The FSPV Operation and maintenance activities are generally more difficult to perform on water than on land. This issue is connected to an advanced workers safety requirements
- System must periodically inspected, reinforced, and replaced to ensure its electrical safety and long-run reliability.
- The FSPV temperature fluctuations may cause floats to blowup and shrink, which can cause cracks. Freezing may stress system components, particularly joints. Additional temperature variations control devices are required with additional costs, etc.

2.4. Shadow effect in solar PV mounting technologies

Many factors influence the performance of a PV system, including environmental factors such as shading, solar radiation falling on it, dust accumulation, module temperature, and solar cell materials. The amount of light that a cell absorbs directly proportions to the amount of current produced by the cell. A reduction in light caused by a lack of sunlight, poles, trees, buildings, passing clouds, dust particles on the panel surface, nearby permanent structures, leaves, birds, and bird droppings falling directly on modules, and the shadow of other panels in its vicinity[23]-[25]. All of these factors contribute to partial or complete shading of a PV module, resulting in a decrease in the current produced by the PV cell. When the current in one PV cell is reduced, the current output of the entire string of series-connected PV cells is reduced, causing the PV panel's output characteristics to change. The reduction in PV system performance caused by shading can be divided into four distinct loss factors: a decrease in incident irradiance on the PV modules, a difference in spectrum between beam and diffuse irradiance, mismatch losses due to varying irradiance and temperature of each cell, and a decrease in inverter MPP tracking due to the I-V curve having false maxima as explored in [23]. Partial or complete shading is the main cause of PV module performance degradation on PV module, the associated effects must be mitigate with different alternative methods towards goods performance of PV module are explained in the following section.

2.5. Mitigation of shadow effect on solar PV and control

The improper operation of a solar cell caused by shadow can be mitigated by the use of a conventional bypass diode, which allows current to flow in the circuit from non-shaded cells. As research advances, newer solutions for reducing the impact of shading, such as DC-DC optimizers or module inverters for adjusting the current reduced from shaded solar cells by lowering the voltage, are becoming available. Because of the presence of shading, multiple local MPP appear in the power curve, misguiding conventional MPPT techniques; to track the global MPP, soft computing-based MPPT techniques are efficient[24].The inverter in a grid-connected PV system is equipped with the MPPT technique, which is primarily used to extract the maximum capable power of the PV modules in relation to solar irradiance and temperature at a given point in time using an MPPT controller[25].

As one method for increasing PV module efficiency, maximum power point tracking (MPPT) techniques are very effective. Incremental conductance (In-Cond), perturbation and observation (P&O), fractional open-circuit voltage (FOCV), fractional short-circuit current (FSCC), fuzzy logic control, and ripple correlation control are all MPPT methods (RCC). The complexity, cost, and popularity of these

techniques vary, as do the rate of convergence, the number of sensors needed, hardware implementation, and effectiveness. Furthermore, these techniques are assessed in terms of varying irradiation and temperature, as well as the calculation of the energy supplied by the entire PV array[26], [27].

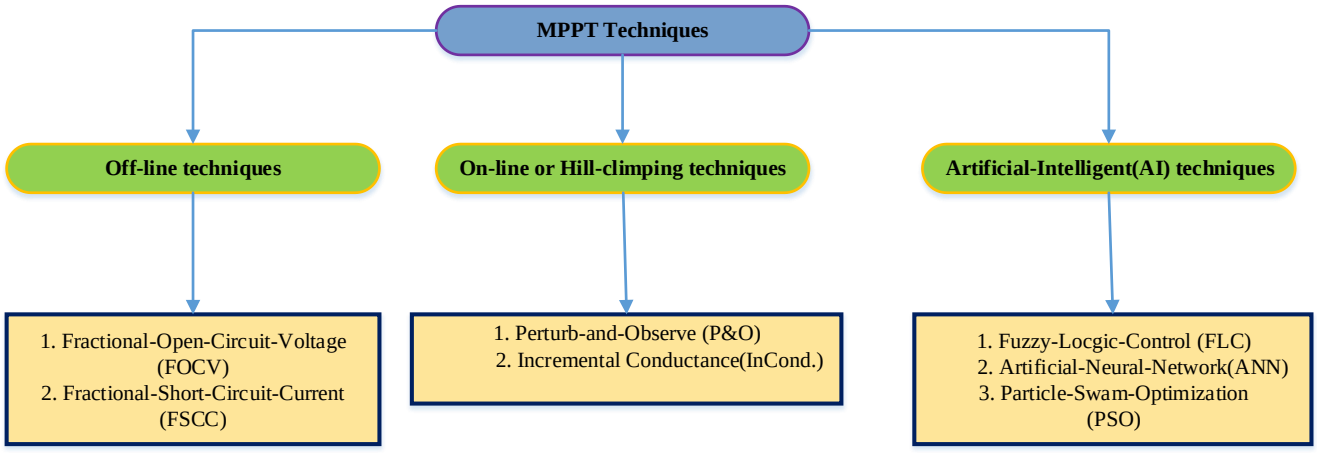

Figure2. 6: Maximum power point tracking (MPPT) techniques[28]

All of the benefits of using the Incremental Conductance method were described in the same study, including its simplicity in implementation, effectiveness, high sampling rate requirement, fast calculation of the power slope, good tracking efficiency, automatic adjustment of the module operating voltage with no oscillations, improved response, and extracted power control optimization. The only negative aspect of the technique is its control unit, which is difficult and expensive to implement, but it is cost effective if implemented using microcontrollers.

In [28], because the author demonstrated that PV power output remains low, ongoing efforts must be made to develop the PV converter and controller for maximum power tracking efficiency and a lower cost factor. Maximum power point tracking (MPPT) is a process that extracts as much power as possible by tracking one maximum power point from array input and varying the ratio between voltage and current delivered. Several algorithms have been developed in order to extract as much power as possible. Due to low PV module efficiency and power failure due to environmental conditions, maximum power point trackers are used to maximize PV module utilization and minimize power failure; Fig.2.6 depicts different types of MPPT techniques used in current PV system technology. The incremental conductance, perturbation, and observation techniques are investigated in this study because they are commonly used in PV system MPP trackers.

2.5.1. Incremental conductance technique

The IC method is based on the fact that the slope of a solar panel's P-V curve (dP/dV) is zero at the MPP, positive to the left of the MPP, and negative to the right, as shown in Fig.2.7[29].

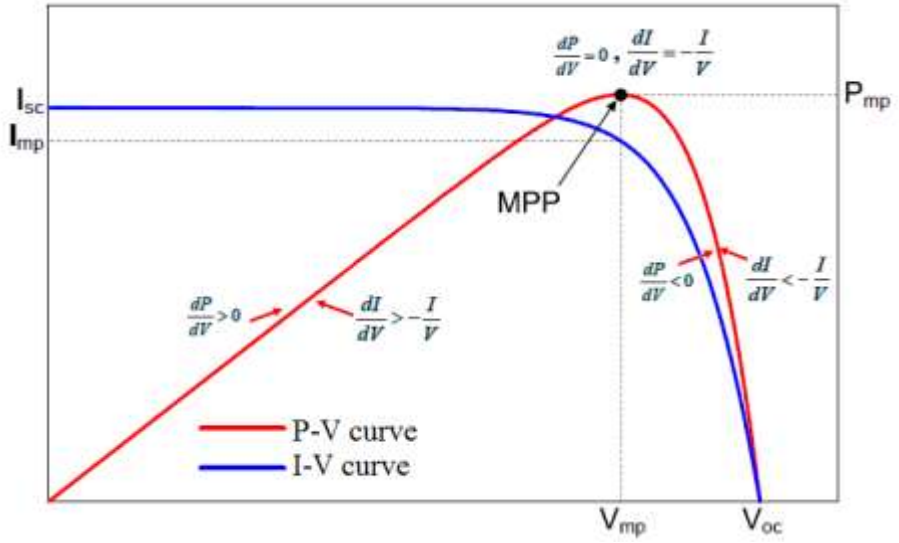

Figure2. 7: P-V and I-V curves of solar panel and signs of its slop at various regions [29]

The Incremental Conductance algorithm uses equation $\left(\frac{dP}{dV}=0\ at\ MPP\right)$ which can be expressed by the voltage and current as below:

$$\frac{dP}{dV}=\frac{d(VI)}{dV}=I\frac{dV}{dV}+V\frac{dI}{dV}=I+V\frac{dI}{dV} \tag{12}$$

At MPP,

$$\left.\frac{dP}{dV}\right|_{\substack{I=I_{mpp}\\V=V_{mpp}}}=0, \qquad \left.\frac{dP}{dV}\right|_{\substack{I=I_{mpp}\\V=V_{mpp}}}=-\frac{I_{mpp}}{V_{mpp}} \tag{13}$$

Where dI/dV_{PV}) represents the incremental conductance (IC) of the solar panel and I_{PV}/V_{Pv} represents conductance. The solar panel will operate at MPP if the ratio of IC equals the negative of instantaneous conductance.

In practice, it is impossible to achieve the equality of IC and negative of instantaneous conductance. As a result, the practical IC method assumes that the MPP is reached when the working point is within a small margin of error (ε).

$$\frac{dP}{dV}=\pm\varepsilon \tag{14}$$

Where ε goes to zero at the MPP.

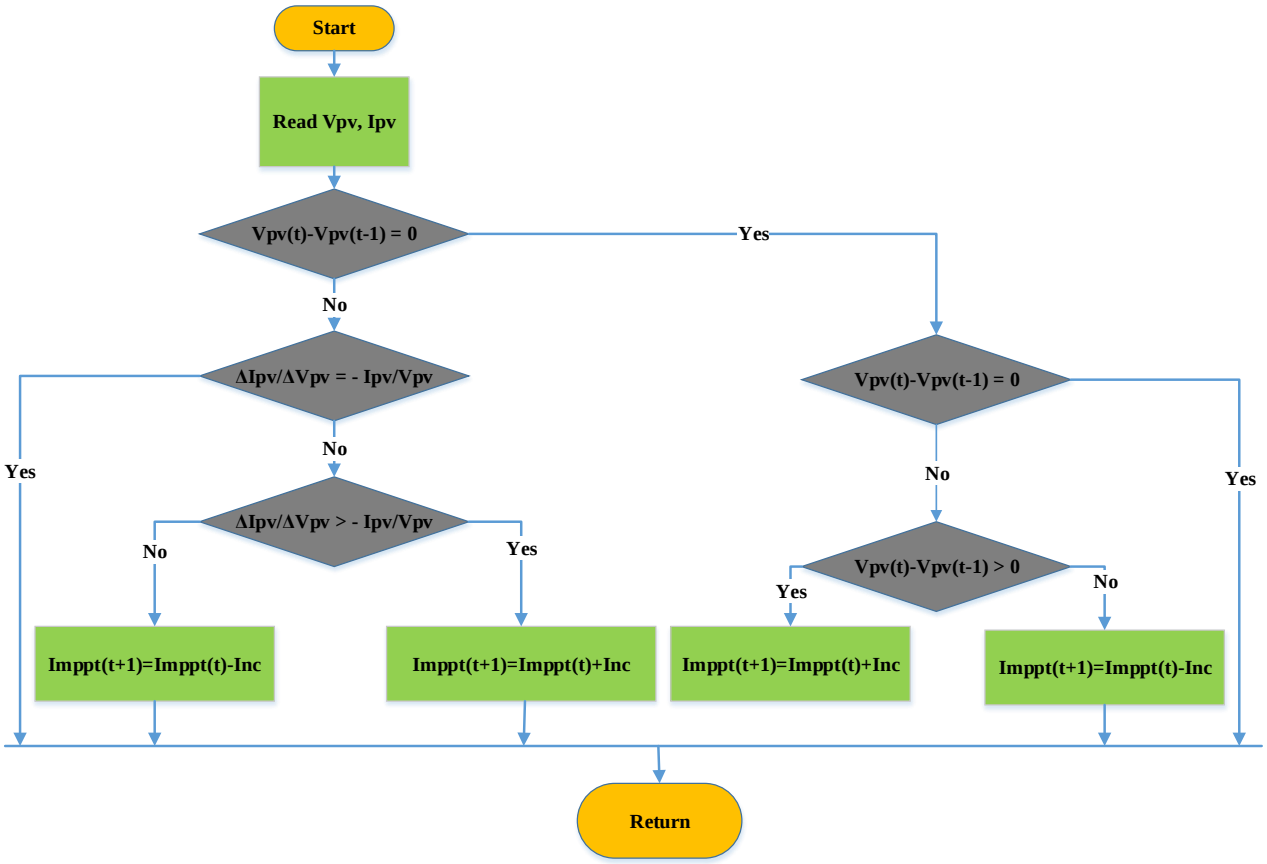

Figure2. 8: Incremental conductance flowchart algorithm [29]

To avoid tracking past the margin, the step size must be smaller than the margin. Furthermore, the incremental variations can be approximated by subtracting the actual values of V_{PV} and I_{PV} in the two subsequent sampling times.

$$\left.\begin{aligned} dI \approx \Delta \mathrm{I} = \mathrm{I(t)} - \mathrm{I(t-1)} \\ dV \approx \Delta V = V(t) - V(t-1) \end{aligned}\right\} \quad (15)$$

Therefore the governing equations become:

$$\left.\begin{aligned} \frac{\Delta I}{\Delta V} = -\frac{I}{V} \quad & for\ V = V_{mpp} \\ \frac{\Delta I}{\Delta V} > -\frac{I}{V} \quad & for\ V < V_{mpp} \\ \frac{\Delta I}{\Delta V} < -\frac{I}{V} \quad & for\ V > V_{mpp} \end{aligned}\right\} \quad (16)$$

The flowchart of the IC algorithm is shown in Fig.2.8

Where: D= is the duty cycle varying from 0 to 1, ΔD= is the change in duty cycle, ΔV= is the change in voltage, ΔI= is the change in current, V_{pv}= photovoltaic panel voltage, and ε= a small marginal error.

2.5.2. Perturb and Observe algorithm

The P&O algorithm is the most widely used and workhorse MPPT algorithm due to its balance of performance and simplicity. However, it lacks speed and adaptability, both of which are required for tracking fast transients in varying environmental conditions. Although it is a simple and straightforward technique, its performance suffers as a result of the trade-off between accuracy and speed when determining step size[27]. To ensure maximum power, this algorithm modifies the operating voltage.

V_{PV}: is the panel output voltage, I_{PV}: is the panel current, P_{PV}: is the panel output power, I_{MPP}: is the panel current at MPP, V_{MPP}: is the panel voltage at MPP, k: is the present time while (k+1): is the future time.

In case where if the output power ΔP is greater than zero for a given increment in V_{PV} (V_{PV}>0), the MPPT moves toward the maximum power point MPP value; if ΔP <0, then the MPPT moves away of the MPP.

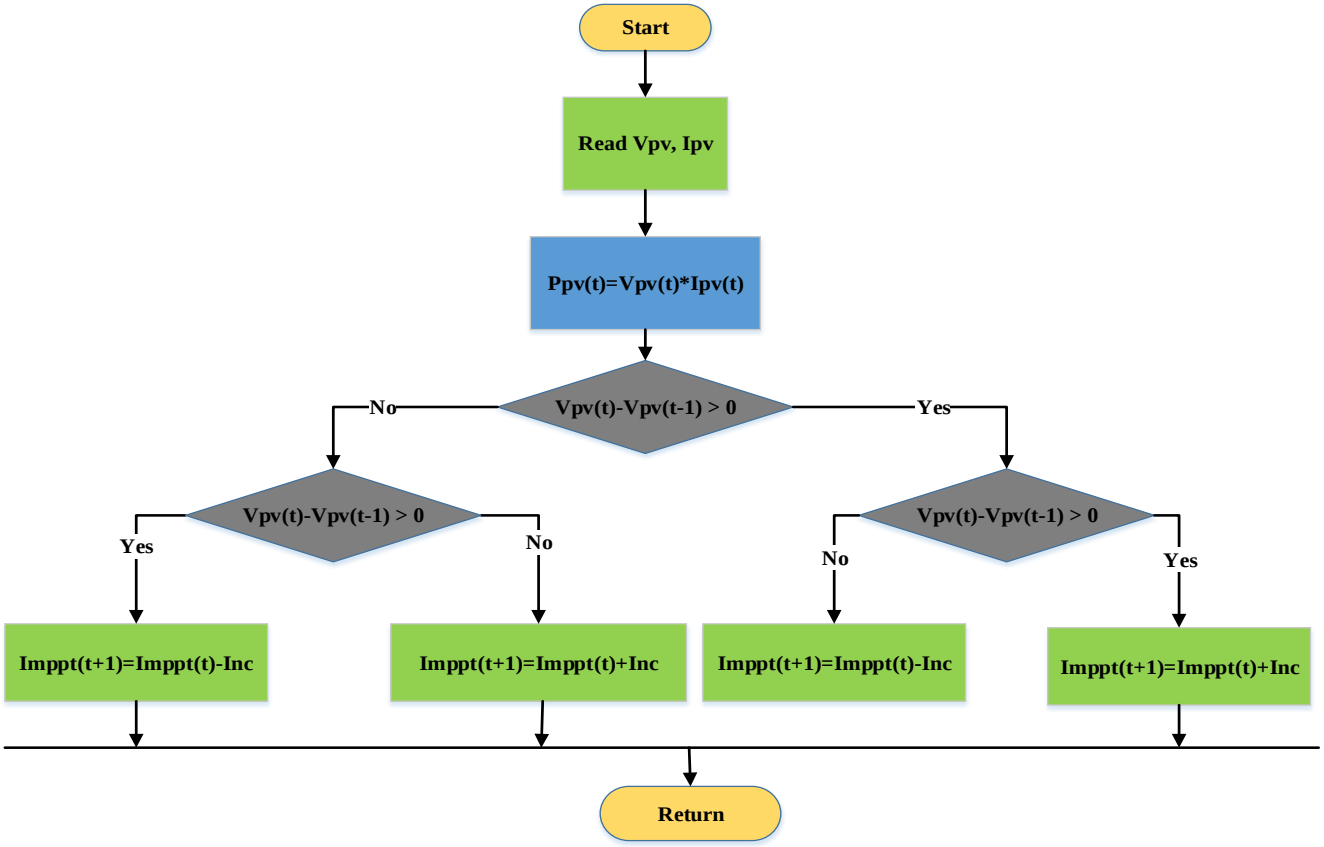

Figure2. 9: Perturbation and Observation flowchart algorithm [29]

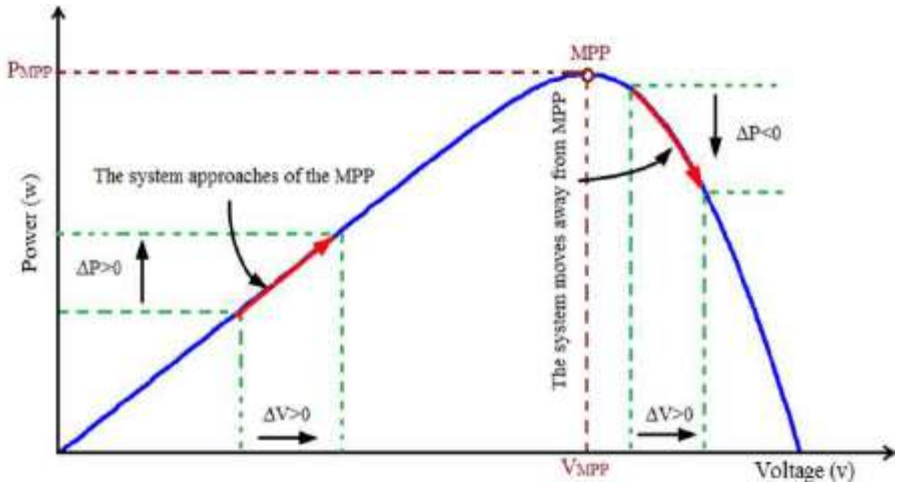

Figure2. 10:Behavior of P&O MPPT algorithm with P-V curve[30]

The control algorithm is shown in Fig.2.10 for each case. In [27], the P&O algorithm is explained as being based on a perturbation of the system's operating point, causing the PV array terminal voltage to fluctuate around the MPP voltage even when the solar irradiance and cell temperature are constants.

2.6. Temperature effect on PV module

In [31], some electrical characteristics of a solar PV cell, such as short-circuit current, open circuit voltage, and power output, are temperature dependent, according to the author. This study discovered that as temperature rises, the short circuit current of a solar cell increases slightly, the open circuit voltage decreases rapidly at a rate of 2.3 mV/^{o}C, and the rate of change in short circuit current increases slightly is 0.1 $Am^{-2o}C^{-1}$, the rate of change in short circuit voltage is$-2.2\ mV^{o}C^{-1}$, the rate of change for maximum output power is$-0.5\%\ ^{o}C^{-1}$. While the power output of the cell decreases at the rate of about 0.6% $^{o}C^{-1}$. Second, as the intensity of illumination increases, so does the short circuit current, up to a reasonable level of illumination. As the intensity of the illumination increases, so does the open circuit voltage. Similarly, open circuit voltage is less sensitive to variations in illumination and illumination level. This means that when cells are exposed to high levels of illumination, it is preferable to provide cooling. This is because the power output of the cell decreases as the temperature rises under high levels of illumination. In [32], the author emphasizes the effect of variation in solar cell operating temperature as a function of solar irradiation level and ambient temperature. Ta, the variable ambient temperature, influences cell output voltage, and photocurrent. The temperature coefficients C_{TV} and C_{TI} for cell output voltage and cell photocurrent, respectively, represent these effects in the model, as:

$$C_{TV} = 1 + \beta_T(T_a - T_x) \quad (17)$$

$$C_{TI} = 1 + \frac{\gamma_T}{s_c}(T_x - T_a) \quad (18)$$

Where: β_T=0.004 and γ_T=0.06 for the cell used and T_a=20^o C, is the ambient temperature during the cell testing, and S_C, is the benchmark reference solar irradiation and level during cell testing.

2.7. Efficiency comparison between FSPV and GSPV

Many researchers claim that FSPV has a higher efficiency than ground-mounted solar PV. In [33], according to the researcher, the average capacity of the floating panel is 11% greater than the average capacity of a solar panel installed on the ground. According to a study conducted in Singapore, the ambient temperature on water is about 1^{o}C to 3^{o}C lower than the adjacent land environment. As a result of this, it was discovered that the module temperature installed on the water's surface decreased by 5^{o}C to 10^o C, resulting in an increase in the energy yield of the installed PV capacity[15]. Furthermore, on open water, the wind speed is higher than on land, which aids in module cooling. Because the tilt angle is kept low to reduce wind loads, and the enterrow shading is also reduced, the FSPV on water bodies is rarely shaded by objects or buildings, which improves the efficiency of the FSPV and distinguishes it from land-mounted solar PV power plants. The energy yield of this new technology, according to the researcher, is 10% higher than that of ground mounted PV systems. Furthermore, a remote sensing method revealed that the lake has a lower temperature than the ground, in terms of prediction, FSPV efficiency was found to be 0.61 percent higher than GPV with only an 8^{o}C difference in annual temperature[15]. The devlopment of different methodologies used to achieve objective of the resaerch are detailed in Chapter III.

CHAPTER III: FLOATING PV SYSTEM DEVELOPMENT METHODOLOGY

3.0. Introduction

To achieve successfully the main objective, and specific objectives of the present work, a detailed methodology was developed. The following section describes in detail the developed methodology.

3.1. Methodology

As the research requires different methodologies to achieve the objectives of the research, in this research the documentation, data collection, modelling, and simulation are the methodologies used to achieve the research objectives as stated in the Fig.3.1.

3.1.1. Documentation

The achievement of the goal of the present research work, documentation has been conducted based some researches, existing research gaps, and the trend in solar PV energy generation is done in this research. Recent published research papers, conference articles, renewable energy books, and scientific reports were used for the same purpose. The documentation was not sufficient to conduct the present research therefore, a site visit at Nyarabarongo HPP was necessary. The following section presents the objective of the site visit.

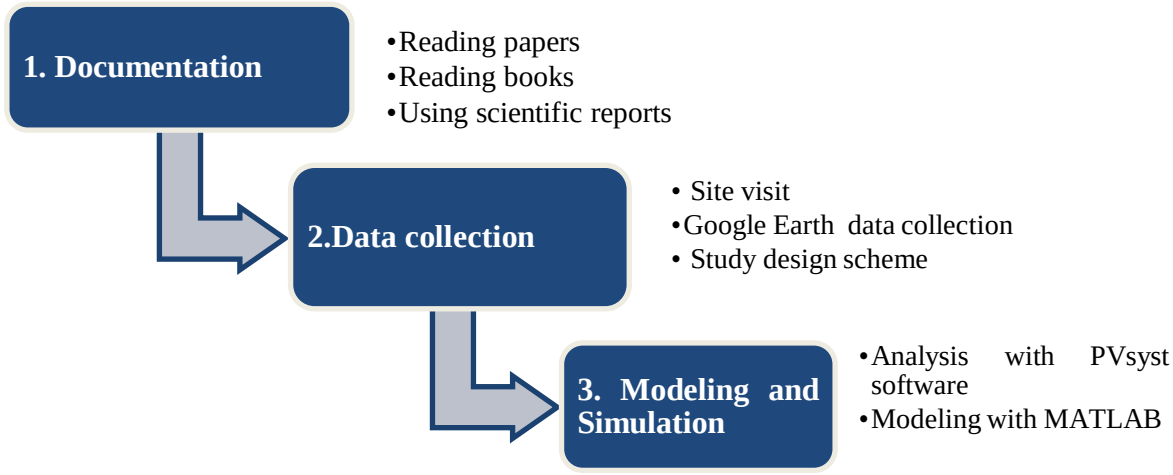

Figure3. 1: Block diagram of Methodology summary

3.1.2. Data collection

The data collection was carried out in order to obtain genuine data. The data was gathered primarily through site visits and Google Earth data related to the Nyabarongo HPP site. The purpose of site visit

is to collect data related to the site technical specifications needed for the system design shown in Table3.1. Google Earth was used to extract the set up and set off of the sun directions at Nyabarongo HPP dam as indicated in Fig. 3.2 from 8h00 AM to 3h30 PM, water is indicated with the yellow color and surrounding mountains with green color. The sun set up from East and set off to West as indicated.

3.1.3. Google Earth data

The surrounding mountains elevations and exact location of the map of the site are shown in Fig 3.3, dam water elevation in Table3.1, altitude, and latitude of the site. Nyabarongo HPP dam water level variation, operating hours of Nyabarongo HPP generating units, Wind speed on dam, dam shadow situation, and the distance between the main roads to the site. The sun set up from East and set off to the West as presented in the Fig.3.2.

Table3. 1: Nyabarongo HPP dam specifications

Item	Specifications
Country	Rwanda
Location	Muhanga District/Mushishiro/Matyazo
Reservoir elevation	1,555 m (5,090 fts)
Turbines	2x14 MW(19,000 hp)
Installed capacity	28 MW (38,000 hp)
Maximum height of the dam	44.5 m
Dam length	230.37 m
Dam head	59.3 m
Length of the reservoir	22 km
Design flood	554 m/sec
Dam type	Concrete gravity
Commission date	2014

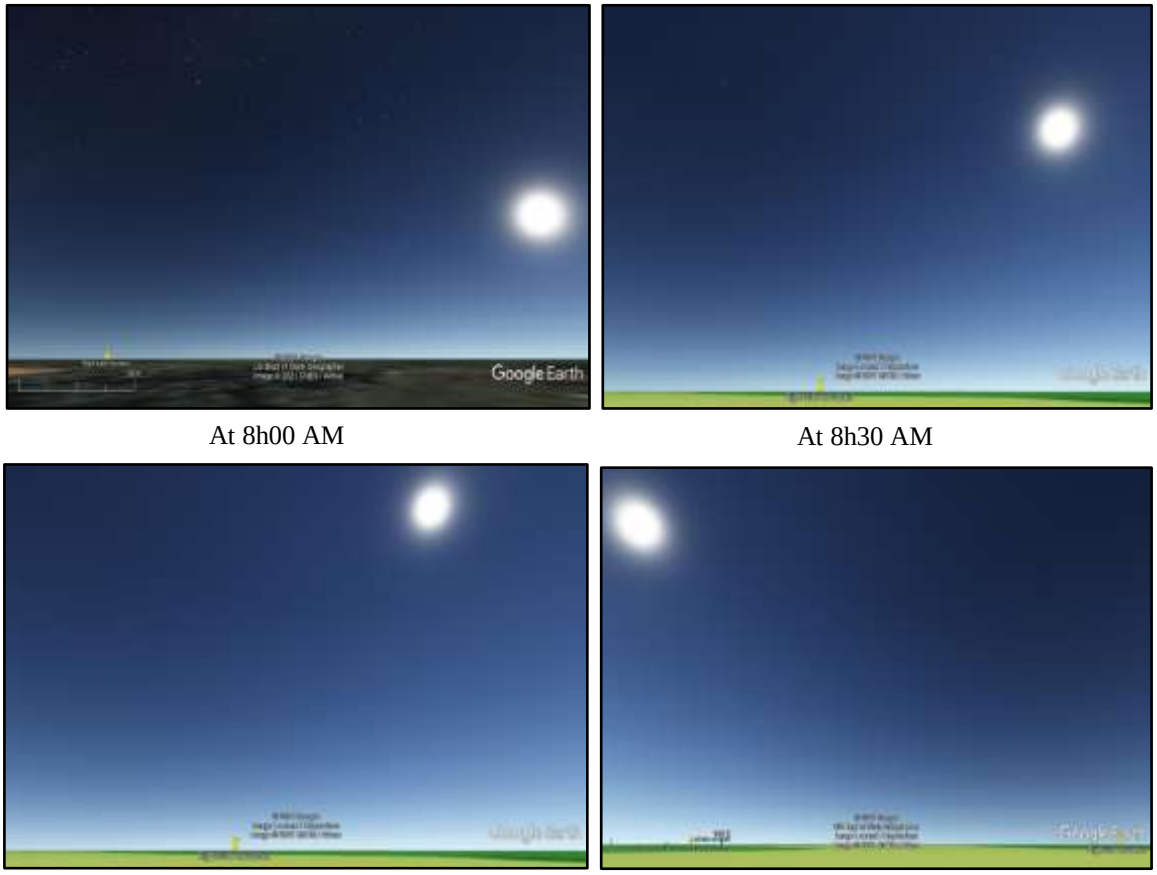

At 8h00 AM At 8h30 AM

At 9h30 AM At 3h30 PM

Figure3. 2: Nyabarongo HPP sun set up and sun set off directions

3.1.4. Nyabarongo HPP dam on a Map (Bijyojyo)

Nyabarongo HPP geographically is located in Rwanda, Western province, Muhanga District, and Mushishiro sector, Bijyojyo and Matyazo cells to Mwogo River. Its reservoir elevation is 1,555 m (5090feets), length of the reservoir is 22 km with concrete dam length of 230.37 m, and with height of 44.5m. The Nyabarongo upper catchment lies within the Nile washbasin and flows from south to north in western Rwanda. It has a surface area of 3,348 km^2, accounting for 12.7 percent of Rwanda's total surface area (26,338 km^2). The catchment is well-known as Rwanda's "water tower," with numerous large tributaries including the Mwogo, Rukarara, Mbirurume, Munzanga, and Satinsyi Rivers. A significant portion of the catchment in the west is at high altitude, above 2,000 m, with steep slopes; the highest point is 2,950 m, as shown on the map in Fig.3.3[34].

(a) Minimum extracted surface on Nyabarongo HPP dam view

(b) Left and Right side mountains view

(c) Nyabarongo HPP dam view

(d) Nyabarongo HPP dam cell location

Figure3. 3: Nyabarongo HPP dam and its cell location on map

3.2. Meteorological data at Nyabarongo HPP dam

The FSPV system is designed based on meteorological data shown in Table3.2, for one year, where, the minimum global horizontal irradiation at the site is 5.06 kWh/m^2/day in June, and the maximum irradiation is 5.83 kW/m^2/day in January. The average ambient temperature is 19.31^{o}C, the average wind speed is 2.15 m/s, and the relative humidity is 74.41 percent. The graph in Fig.3.4 depicts the change in global horizontal irradiation, horizontal diffuse irradiation, temperature, wind velocity, and relative humidity at the site.

Table3. 2: Meteorological data variation at Nyabarongo HPP dam

Months	Global horizontal irradiation (kW/m^2/day)	Horizontal diffuse irradiation(kW/m^2/day)	Temperature (oC)	Wind velocity (m/s)	Relative humidity in%
January	5.83	2.25	19.6	1.9	75.4
February	5.69	2.26	20.1	2.1	73.5
March	5.61	2.37	19.8	2	75.5
April	5.4	2.28	19.1	1.99	79.7
May	5.25	2.12	19.4	2.09	76.3
June	5.06	1.85	19.1	2.39	69.8
July	5.33	2	18.7	2.6	68
August	5.28	1.97	19.2	2.5	70.3
September	5.26	2.36	19.1	2.39	73.9
October	5.28	2.58	19.6	2.2	74
November	5.47	2.2	18.9	1.9	78.9
December	5.52	2.34	19.1	1.79	77.6
Average	**5.42**	**2.22**	**19.31**	**2.15**	**74.41**

3.2.1. Nyabarongo HPP dam and Power house technical data

To design the FSPV on Nyabarongo HPP dam, it is mainly required to have the technical specifications of the existing HPP: The transformer information, generation capacity, frequency and operating voltage and other technical specifications are the prerequisite to start the modelling and simulation of the FSPV system.

Table3. 3: Nyabarongo HPP technical specifications

Items	Values
Transformer	2*16.5 MVA/2*14,000kW/6.6kV/110kV
Generator max current	1,400 A
Generator overcurrent	1,700 A
Minimum generator voltage	6.6-7.2 kV
Nominal frequency	50 Hz
Under-frequency	47 Hz
Over-frequency	52 Hz
Maximum reactive power/Gen.	11 MVA
Power factor range	0.85-1 Lagging
Minimum of dam water level	1,495 m
Maximum of dam water level	1,499 m
Maximum production of two generators	28 MW
Minimum production of two generator	20 MW

Therefore during the site visit, it was necessary to collect data related to Nyabarongo HPP and sun direction for solar irradiation potential at the site as indicated in Fig.3.2. Table3.1 presents different nominal values of various equipment at Nyabarongo HPP.

3.2.2. Installed power at Nyabarongo HPP

Based on monthly report, in July/2021, the total energy generated by generating unit I is 4,217.50 MWH of energy, while generator unit II generates 1,511.70 MWH as indicated in Fig.3.4.

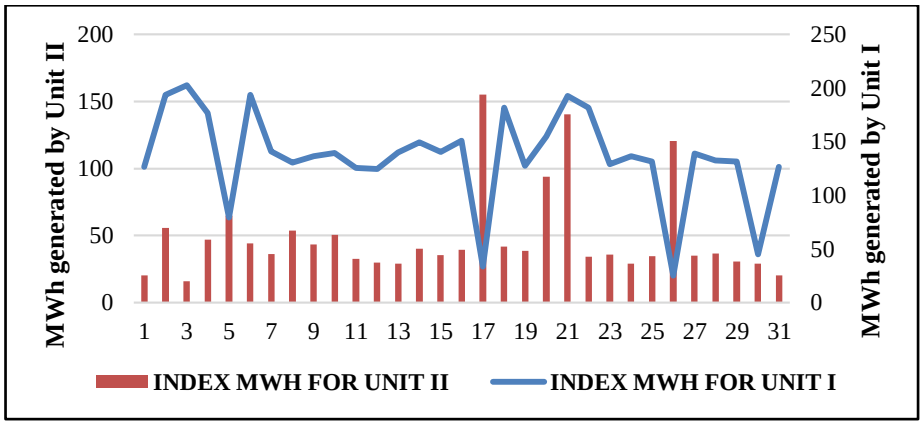

Figure3. 4: Nyabarongo HPP MWh index for unit I& II for Month of July/2021

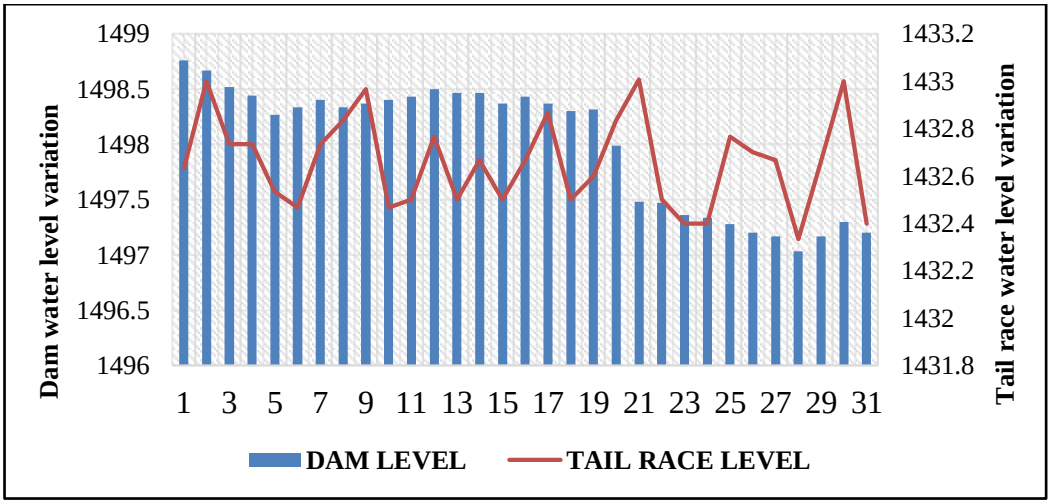

Figure3. 5: Month of July /2021dam water level and tail race level

The variation of water level in this month was not significant as indicated in Fig.3.5. To install the FSPV on Nyabarongo HPP dam targets the compensation of water level variation pertinently for the sunny period which causes water evaporation and leading to instability of HPP generation capacity.

3.3. Modeling and simulation

The potential power of FSPV system was modeled and simulated using PVsyst software .To validate the results from PVsyst, simulation, and harmonics analysis have been done using Matlab software. The used data in these software were based on the standards of PV and best performance of PV panels on the market. The details, description of the simulation, and harmonics analysis due to FSPV integration with the grid and the harmonics due to the grid interconnection with FSPV are in the next Chapter.

CHAPTER IV: FLOATING PV SYSTEM MODELLING AND SIMULATION AT NYABARONGO HPP DAM

4.0. Introduction

As modeling requirements for other systems, FSPV study requires a good mathematical modeling. The modeling has considered the data collection presented in the previous chapter. It puts into consideration the case study as well. The first part of modeling investigates the potential power production of the site using PVsyst software. Secondly, mathematical modeling was done and finally, the simulation of the FSPV on Nyabarongo HPP dam was conducted to validate the modeling concept by using MATLAB software. The FSPV system, and DC-AC inverter nominal values were calculated using PVsyst software. DC-link between the FSPV and the DC-DC converter were modelled and sized to meet the system requirements. The simulation considers the existing technical specifications of Nyabarongo HPP given in the Table 3.1 in the previous chapter. Moreover, the data of the site and design scheme described in the following section are considered as well to prove the potential power generation at the site from FSPV.

4.1. Study design scheme

The design schemes comprises different parts of the FSPV topology on which the simulation is based on. The Fig.4.1, gives a brief detail about the research study scheme, from the energy generation source, which is FSPV, feeding its output voltage, and current to DC-DC boost converter connected to DC-AC inverter that converts DC voltage or current into alternating voltage and current before being stepped up by a transformer and connect it to Nyabarongo HPP substation bus and delivers to National grid. The voltage and current control techniques done at the level of DC-DC boost converter and inverter are shown in Fig.4.2.

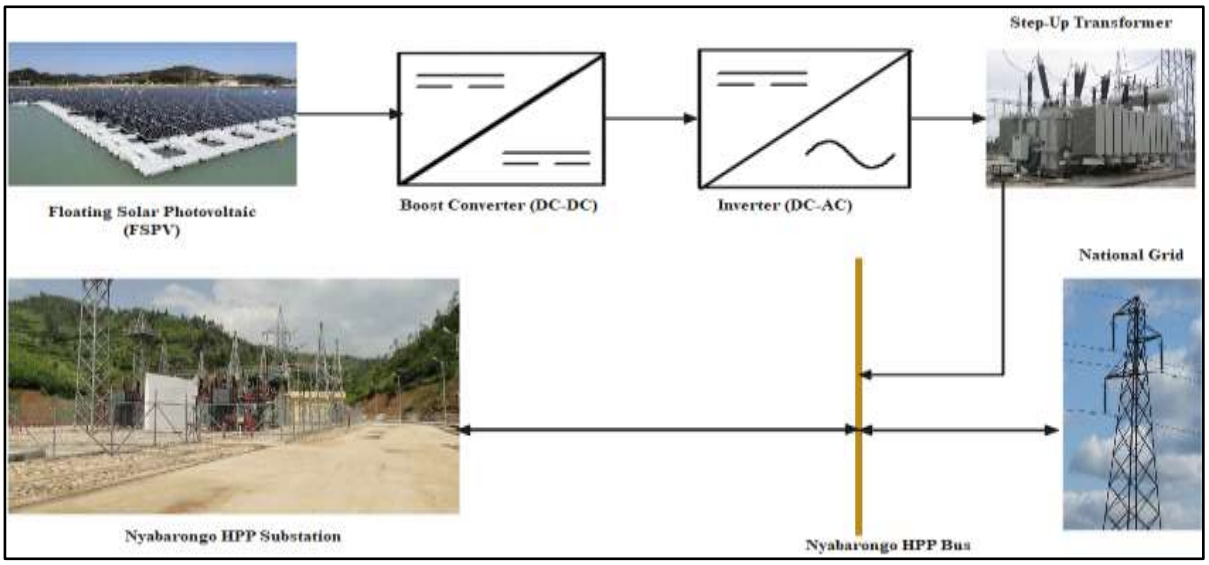

Figure4. 1: Block diagram of the proposed system

Figure 4.1, there is no closed loop block diagram. However, the FSPV must have a closed loop system to ensure system stability. The Maximum Power Point Tracking (MPPT) algorithm provides the maximum power point for any change in operating conditions of the FSPV system, which is achieved using the Incremental Conductance (IC) method, as shown in the block diagram of Fig.4.2. A DC-DC boost converter also ensures that the output voltage is always greater than the grid peak voltage[35],[36]. There is also a DC-AC inverter and control unit that provides an AC voltage that meets the grid requirements for connection and synchronization. The functionality of the system's controllability takes into account the solar irradiance at the site, as described in section 4.2.

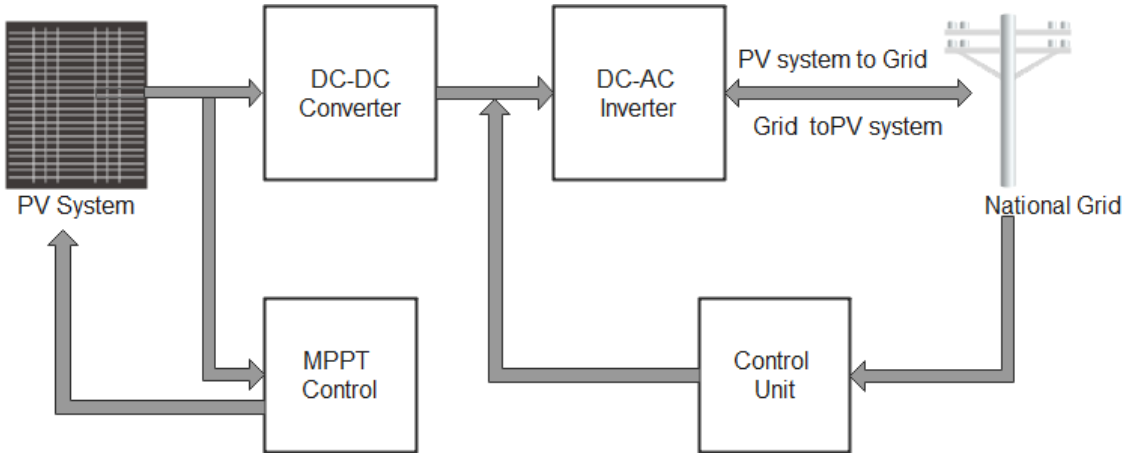

Figure4. 2: Block diagram of a general Grid-connected PV system with control [33]

4.2. Solar irradiance at the site

The National Aeronautics and Space Administration (NASA) of the United States and the University of Rwanda assessed Rwanda's solar radiation and solar resources. Rwanda's Southern Province has global horizontal irradiance ranging from 5.2 to 5.4 kWh/m^2, while the East Province has the greatest potential for solar energy generation. Another academic study, conducted in 2007 in collaboration with the Ministry of Infrastructures (MININFRA) department of meteorology, used a meteorological data set to estimate monthly averaged global solar radiation. In Rwanda's Southern and Eastern provinces, daily solar irradiation ranges from 4 kWh/m^2 north of the city of Ruhengeri/Musanze to 5.4 kWh/m^2 south of the capital, Kigali. However, conditions vary seasonally, with average daily irradiation levels in the cloud reaching about 4.5 kWh/m^2, and the total annual potential estimated to be around 66.8 TWh[1]. This fluctuation is governed by the previously mentioned control. As shown in Fig.4.3, the Nyabarongo HPP dam, a case study of the research, is located in Muhanga District. Figure 4.4 depicts its solar irradiance behavior.

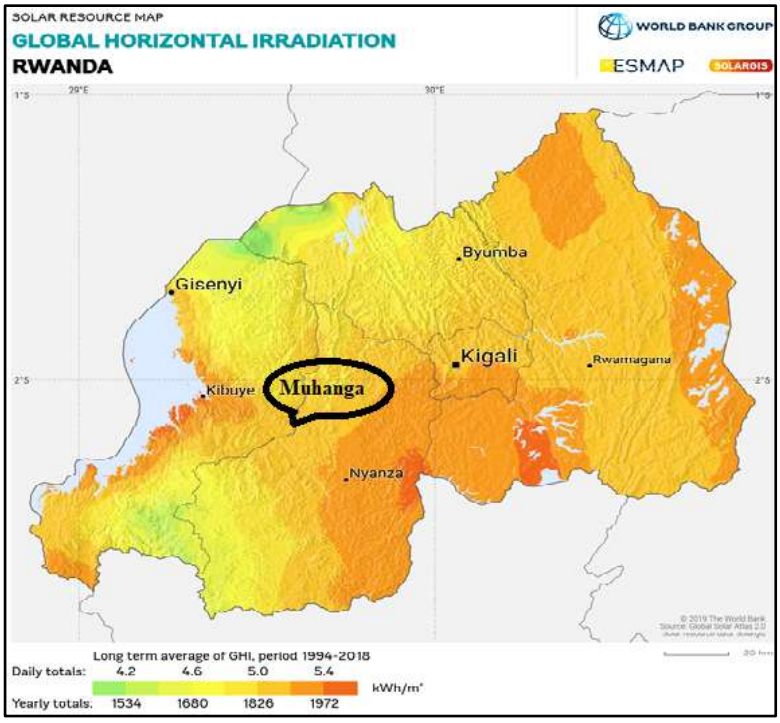

Figure4. 3: Global horizontal irradiation map for different districts of Rwanda

On Fig.4.4 (a), the power generation capacity per m^2 in a day always depends on ambient temperature of the site, at 18.28^o C; the global horizontal irradiation, horizontal diffuse irradiation, and horizontal global clear sky model were found to be 7.573 kW/m^2/day, 1.087 kW/m^2/day, and 8.11 kW/m^2/day respectively as indicated in Fig4.4 (a).

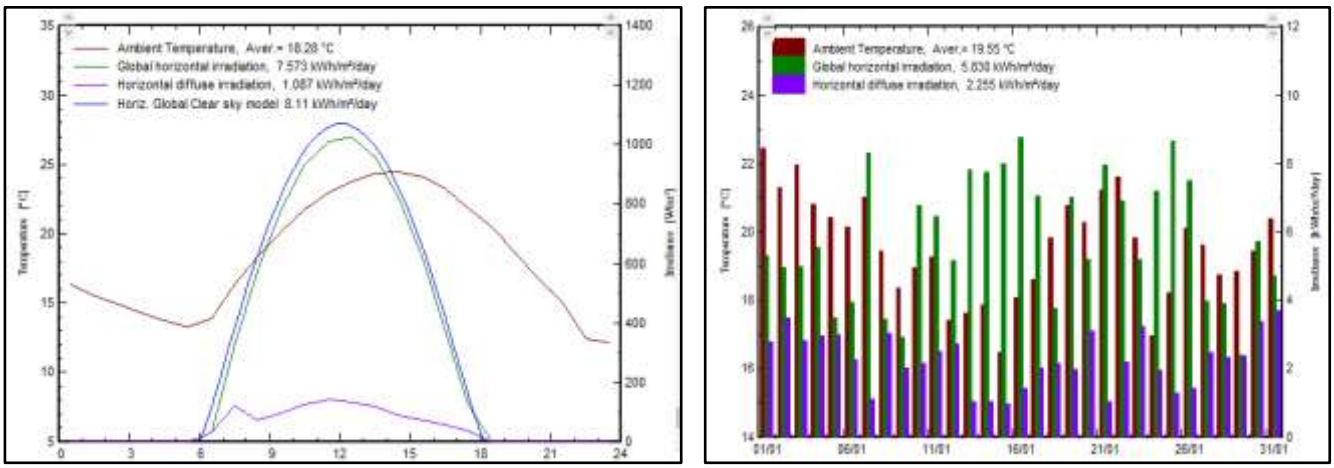

(a) (b)

Figure4. 4: Irradiance in in kW/m^2/day at different ambient temperatures

At ambient temperature of 19.55^{o}C the global horizontal irradiation and horizontal diffuse irradiation become 5.830 kW/m^2/day, and 2.255 kW/m^2/day as shown in Fig.4.4 (b).

The efficiency of the system is not only affected by the irradiance but also it is influenced by relative humidity and wind velocity as indicated in Fig.4.5. The relative humidity average and wind velocity average are respectively 74.41%, and 2.15m/s^2. Some factors affect positively the PV system, other affect it negatively. Therefore, analyzing of losses based on different factors is useful. The researcher in [37], demonstrated that, the moderate wind improve the efficiency of the PV system due to its cooling effect on the PV system. But the high relative humidity increases the shunt resistance of the PV cell which affects the output power of PV system negatively. The high relative humidity lower global horizontal irradiance which affects the efficiency of the PV system negatively as indicated by the Fig.4.6. For good performance of PV system, it is required to operate at moderate wind speed and low humidity. In the Fig.4.7; the array normalized production, normalized array loss ratio, normalized system production, and the normalized system loss ratio are indicated such as 4.8kWh/kWp/day, 1.25, 4.43kWh/kWp/day, and 0.077 respectively.

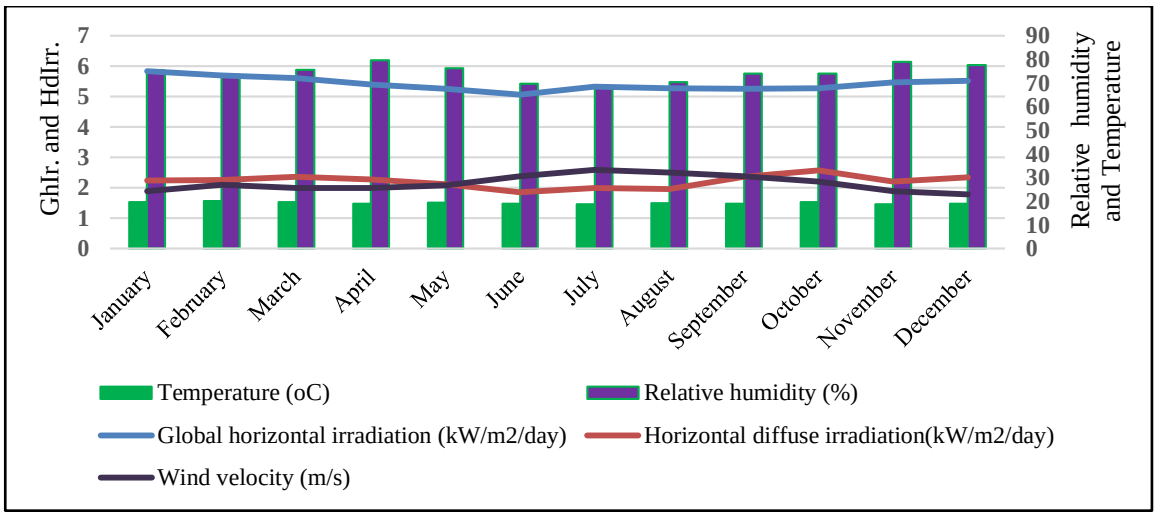

Figure 4. 5: Nyabarongo HPP dam Meteorological Data

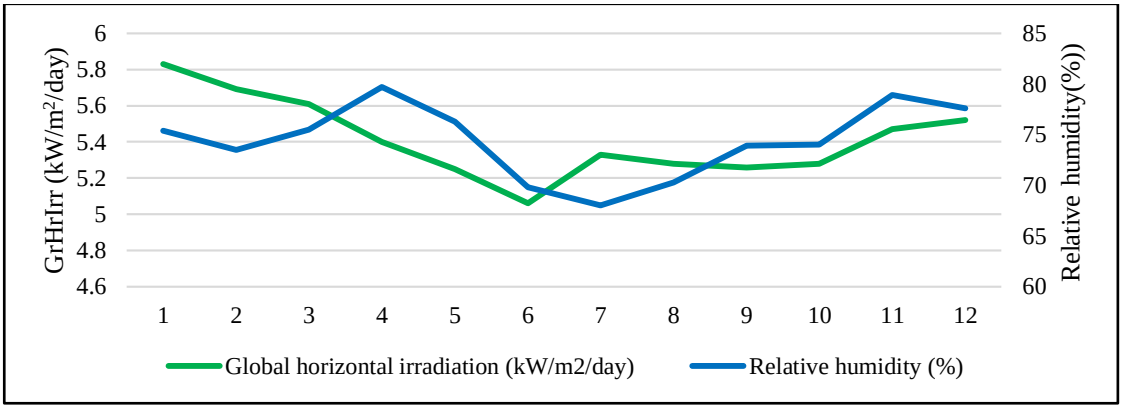

Figure4. 6: The effect of relative humidity on global horizontal irradiance

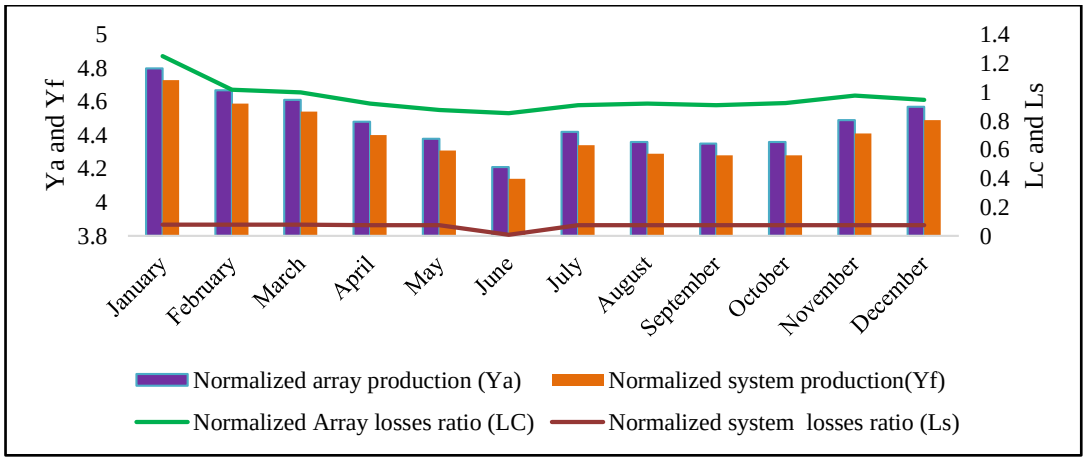

Figure4. 7: Normalized array system production and related losses ratio

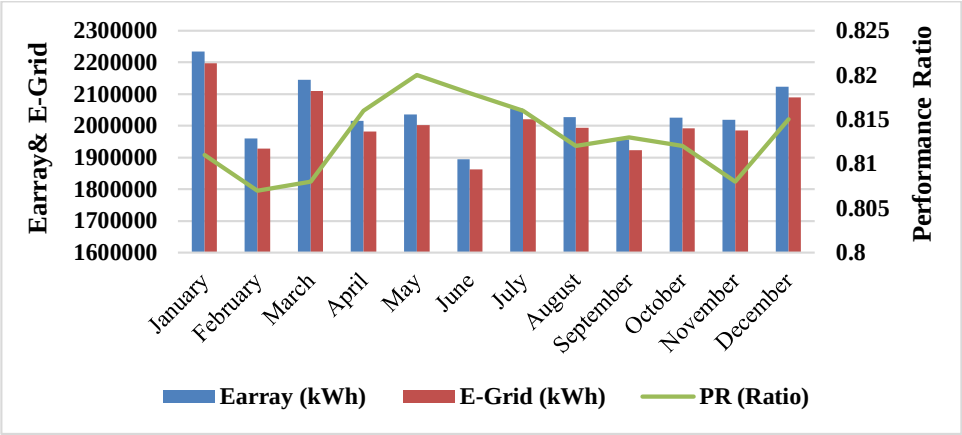

Figure4. 8: Array energy and injected energy into the grid with performance ratio

4.3. FSPV potential power at Nyabarongo HPP dam

The FSPV potential power was estimated using PVsyst. Data collected from the site in Table3.1 were used to simulate the number of the modules and surface used for FSPV model are 33,750 module area of 72,970 m^2, 5 inverters, nominal PV power output of 15,019 kWp, maximum PV output power of 15,506 kWDC, nominal AC power of 15,000 kWAC and nominal power ratio of 1.001. This research work is partially based on the PVsyst software. The PVsyst have been used for modeling purpose. All the figures, tables depicted here in this research are generated during the simulation process for Nyabarongo HPP dam site. The results from extracted surface part of the dam water were indicating that the site has greater power potential, the yearly energy produced is 24,087 MWh/year, the specific production is 1,604 kWh/kWp/year, the normalized production is 4.39kW/kWp/day, and performance ratio of 81.2% as shown in the Fig.4.8.

4.3.1. System losses

Various losses area available for the whole FSPV system such as near shading loss, PV conversion loss, boost converter loss, inverter loss, and ohmic loss. The near shading loss is due to the surrounding mountains, Matyazo mountain in East and Bijyojyo mountain in West of the Dam as shown in Fig.4.9

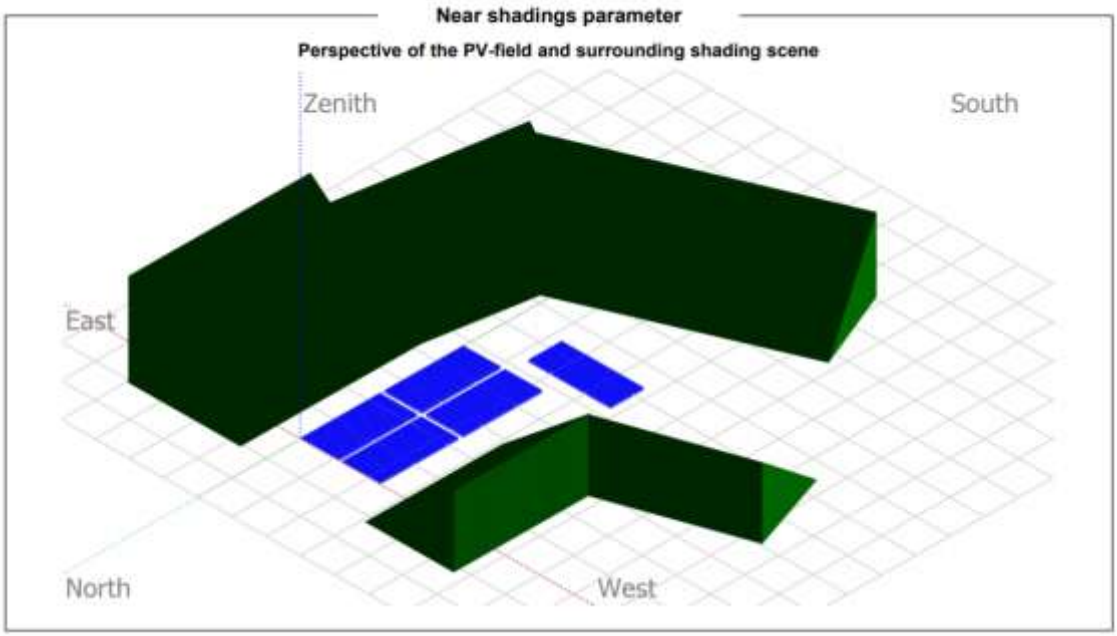

Figure4. 9: Near shading modeling in PVsyst software

4.3.2. Detailed Inverter energy output and losses

The output energy of the inverter, inverter global loss, inverter loss during its operation, inverter loss due to its threshold power, and its efficiency plotted in Fig.4.10 and Fig.4.11 are 24,088,671.0 kWh/year, 403,373.0 kWh/year, 401,369.0 kWh/year, and 768.6 kWh/year respectively.

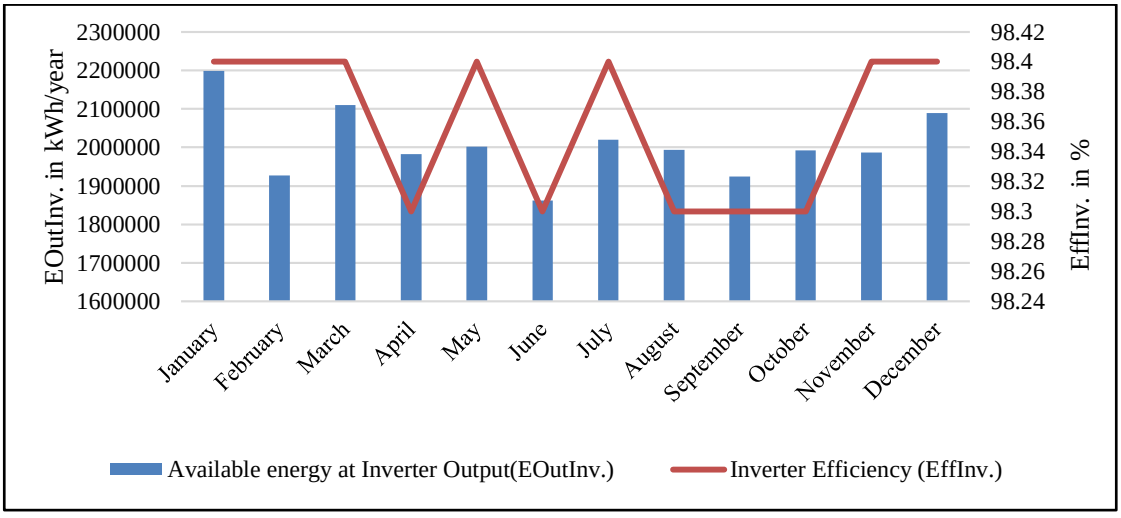

Figure4. 10: Inverter available output energy and its efficiency

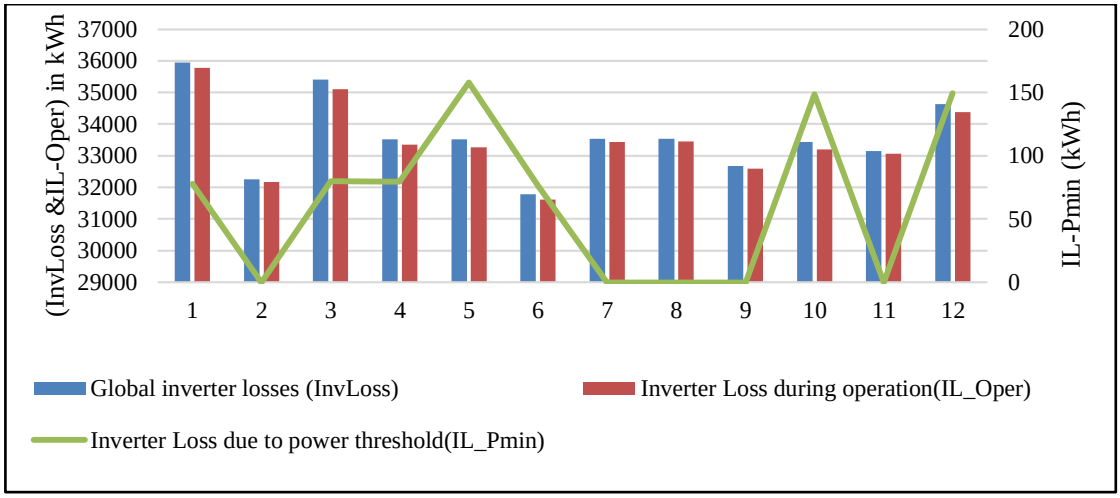

Figure4. 11: Inverter losses

The site is potential and an energy developper can exploit the site using the FSPV. However, a feasability study is required to interface the FSPV and the existing hydropower plant. Therefore, the present research shows how the FSPV can be integrated to the HPP.

4.4. Modelling of power electronic converters for the grid connected FSPV

Since the FSPV is intermittent energy source due to the weather conditions, a power electronic interface is needed to control the voltage, power, and frequency of the inverter. Therefore, proper PV modules for FSPV arrays, a well-designed boost converter with MPPT control is required for FSPV for boosting the PV arrays output voltage, and a grid connected inverter well designed with current and voltage control to meet the grid requirement has to be incorporated to interface the FSPV and the grid or Nyabarongo HPP, finally, the inductor (L), capacitor (C), and inductor (L) filter to suppress harmonics from inverter must be added to the output of the inverter.

4.4.1. PV module technical specifications

For this modeling, a Sunpower-SPR-445NJ-WHTD.PAN, Si-mono-crystalline PV module is used; the sub-array contains 675 parallel strings and 10 series-connected modules per string. Table4.1 contains additional technical specifications for the selected modules.

Table4. 1: Sun Power SPR-445NJ-WHTD.PAN technical specifications

Parameters	Abbreviations	Values	Units
Module open-circuit voltage	V_{oc}	90.5	Volts (V)
Temperature coefficient of Voc	-	-0.29101	%/°C
MPP voltage	Vmpp	76.7	Volts (V)
Module short-circuit current	Isc	6.21	Amps(A)
Temperature coefficient of Isc	-	0.013301	%/°C
MPP current	Impp	5.8	Amps (A)
MPP Power	Pmpp	444.86	Watts(W)
Number of cells per module	128	-	-
Diode saturation current	I_o	1.35552e-11	Amps (A)
Light generated current	I_L	6.2167	Amps (A)
Number of sub-arrays	-	5	-

4.5. Modeling of DC-DC converter for FSPV

The potential power at the Nyabarongo site is taken into account when sizing the DC-DC boost converter. In other words, the power stage and control of the DC-DC boost converter are modelled in accordance with the technical specifications of the FSPV chosen for the site. To minimize switching losses, heat, avoid acoustic noise, reduce inductor and capacitor size, and increase boost converter efficiency, the appropriate parameters, such as input voltage to the converter (V_{inv}), output voltage (V_o), duty cycle (D), switching frequency (fs), and inductor value, must be included in its design for PV system MPPT.

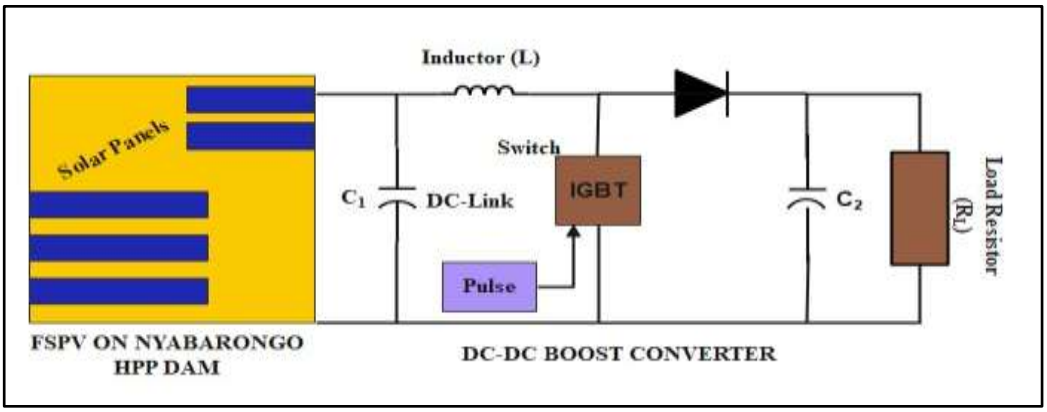

Figure4. 12: DC-DC Boost converter electric circuit

The electric circuit of Fig.4.12 depicts the boost converter model circuit. Equation (19) connects the output voltage and input voltage:

$$D = 1 - \frac{V_{in}}{V_o} \times \eta \tag{19}$$

The proper inductor is selected by using the equation (20) by considering the voltage ripple (ΔV) as 1% and the ripple current (ΔI) as 5% at maximum input voltage.

$$L = \frac{V_{in}(V_{out} - V_{in}) \times D}{\Delta I_L \times f_s \times V_{out}} \tag{20}$$

To ensure the boost convverter continuous conduction mode , the minimum inductor must be selected using equation(21):

$$L_{min} = \frac{D(1-D)^2 R_o}{2 \times f_s} \tag{21}$$

The capacitor value selected is calculated from the variation in output voltage or ripple voltage, it is given from equation (22):

$$C_2 = \frac{D}{R_0 \times f_s \times \Delta V_o} = \frac{D}{R_0 \times f_s \times 0.01} \; or \; C_2 = \frac{I_o \times D}{f_s \times \Delta V_o} \tag{22}$$

The bost converter designed is effective if the parameters values are calculated as indicated in Table4.2.

4.5.1. Boost converter power stage sizing

The following table shows the boost converter design parameters:

Table4. 2: Boost converter design parameters

Parameters	Abbreviations	Values	Units
Input voltage	Vs	767	Volts (V)
Input current	Is	3915	Amperes(A)
Output voltage	Vo	900	Volts (V)
Output current	Io	1564.537	Amperes(A)
Inductor	L	3μH	Henry(H)
Capacitor	C	1mF	Farads(F)
Duty ratio	D	16	%
Efficiency	H	98.5	%
Switching frequency	Fsw	25,000	Hz
Load	R_L	0.575	Ω

The ripple current and ripple voltage are set to 20% and 1%, respectively, to reduce voltage and current ripples at the boost converter's output. The boost converter's efficiency is assumed to be 98.5 percent.

4.5.2. Boost converter simulation

To show the performance of the FSPV is simulation using Matablab was conducted, Fig.4.13

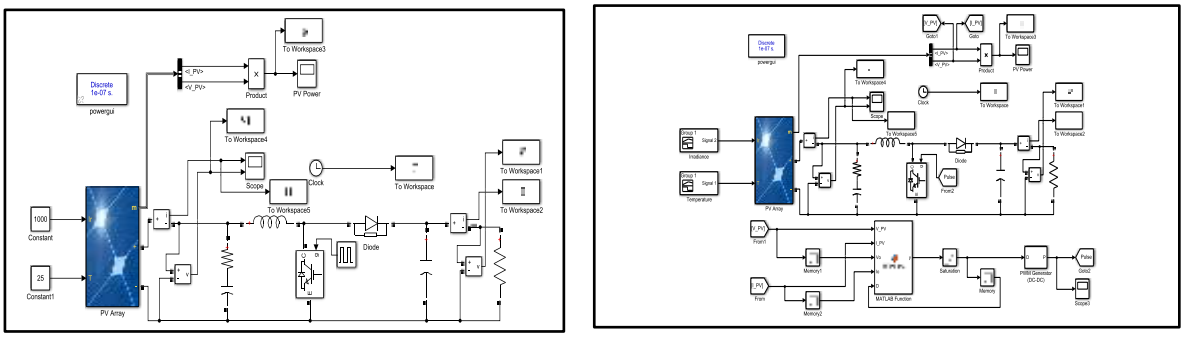

(a) Boost converter open loop

(b) Boost converter closed loop Matlab model

Figure4. 13: Boost converter open loop and closed loop Matlab models

The open loop boost converter simulation in Fig. 4.13 (a) aims to depict the converter's steady state in the absence of feedback control. This provides a starting point for tuning control parameters for the boost converter with a closed loop system see Fig.4.13 (b). The MPPT control takes into account the PV array output voltage behavior shown in Fig. 4.15(a) and (b). The maximum power can change depending on the irradiance value.

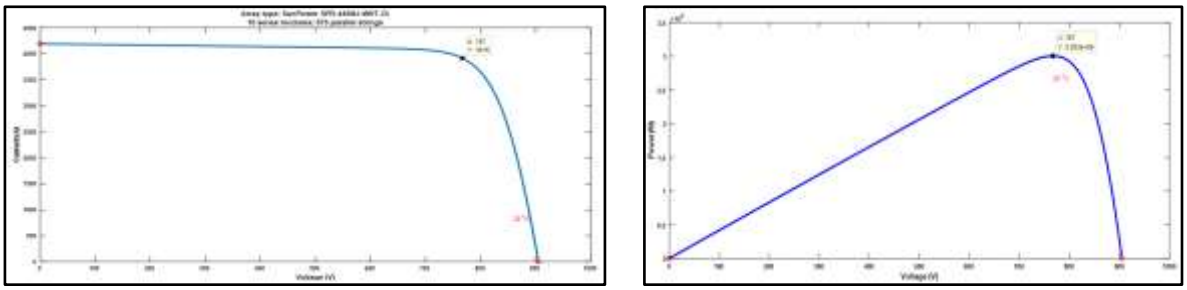

(a) Array output current vs voltage

(b) Array output power vs voltage

Figure4. 14: The PV output voltage, current and power as input to the boost converter

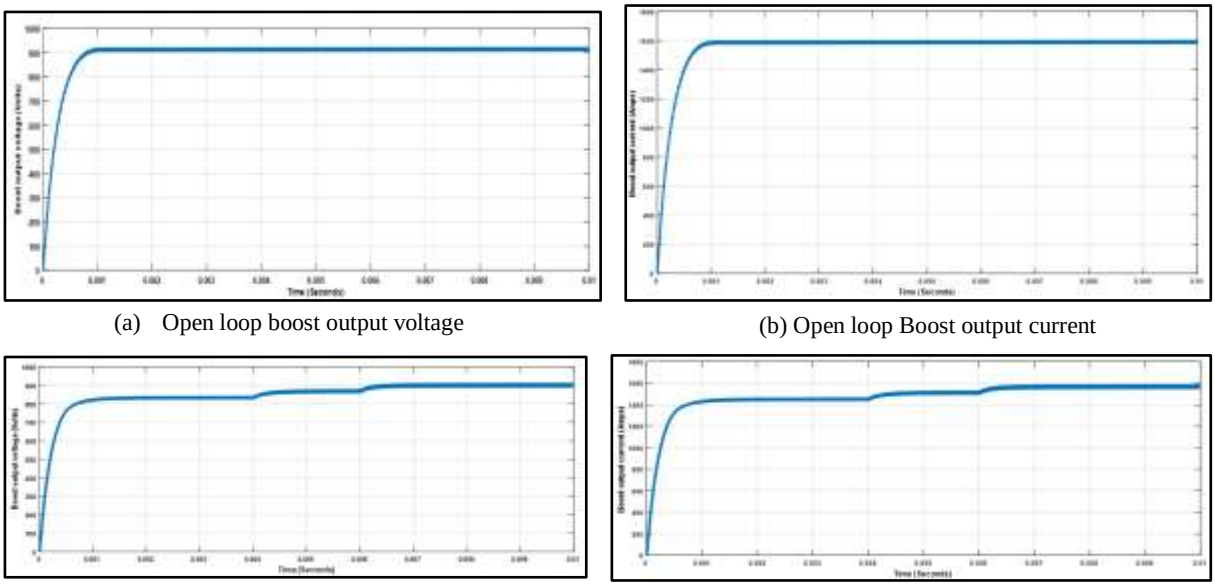

(a) Open loop boost output voltage

(b) Open loop Boost output current

(c) Boost closed loop output voltage

(d) Boot closed loop output current

Figure4. 15: Boost Open loop and closed loop simulation results

The 10 series modules and 675 parallel strings of FSPV inputs the maximum peak voltage of 767 volts to the open loop boost converter as indicated in Fig.4.14 (a), and power of 3,000 kW in (b). The open loop boost converter with 16% of duty cycle, its output voltage was found to be 900Volts, and the current of 1,600A as shown in Fig.4.15 (a), and (b). While the closed loop boost converter voltage output voltage measured is 900Volts as indicated in Fig.4.15 (d). MPPT control the voltage and current are maintained to the same values if there is any change in FSPV operating parameters.

4.6. Modeling of grid connected inverter for FSPV

In this simulation, a Delta solutions India DelCen3000 inverter was used. Table4.2 lists the critical technical specifications of the chosen inverter:

Table4. 3: Design specifications of the inverter

Parameters	Values
Inverter input DC-voltage	900 Volts
Inverter output AC-voltage	400 Volts (rms)
Inverter operating DC-voltage	630-930 Volts
Inverter power rating	3 MWac
Switching frequency	25 kHz
Inverter efficiency	98.69%
Number of sub-arrays	5
Number of MPPT per inverter	24
Number of inverter needed	5
Total Power injected in the grid	15 MW

4.6.1. Grid connected inverter control scheme for FSPV

Because the DC-DC converter was modeled using the FSPV technical values, the inverter is also modeled using the same values. However, the inverter modeling is based on the output of the DC-DC converter. The inverter's stability is implied by the stability of the DC-DC converter. As shown in Fig.4.16, the inverter current and voltage were controlled. The DC-link voltage is set in accordance with the PV output power. The boost converter output serves as the reference for the active current controller (I_{dref}), while the reference for the reactive current controller (I_{qref}) is set to zero because the photovoltaic system connected to the low voltage distribution network is expected to deliver only active power under normal conditions. As a result, the current vector is always in synchronization with the grid voltage. In order to control a three-phase grid-connected inverter, the inverter voltage, and current must be sensed, as shown in Fig.4.17. The design of a three phase grid connected inverter is based on the design of its filter and controller. The PLL is there to synchronize the inverter output with the grid with respect to common voltage, voltage phase angle, and same frequency with the grid.

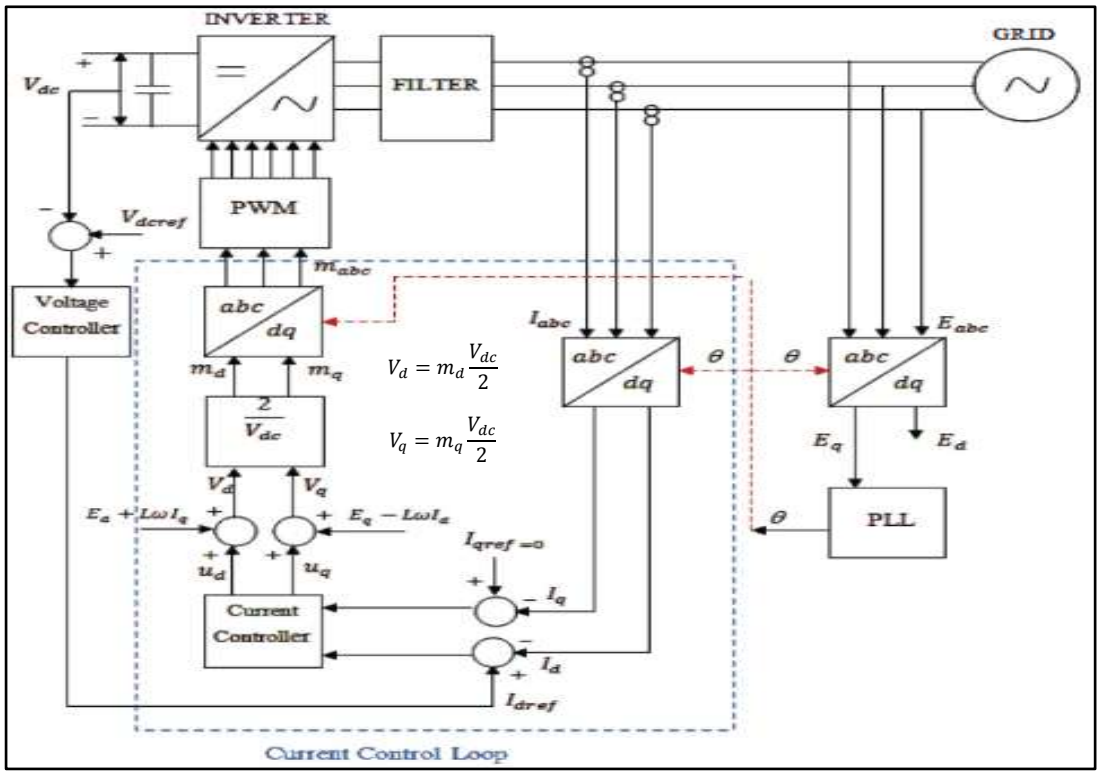

Figure4. 16:Grid connected inverter dq-control scheme [38]

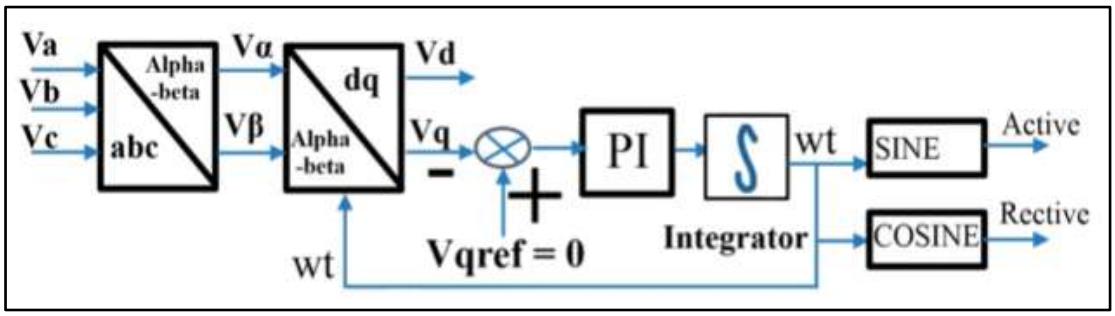

Figure4. 17:PLL Closed loop model[39]

Due to power electronics switching device, the inverter can cause some harmonics on the side of the grid. To minimize these harmonics, the LCL filter is strong enough to suppress them at high level.

4.6.2. Grid connected inverter LCL filter modelling for FSPV

The preliminary goals of three phase LCL filter design are to reduce voltage and current distortion, to alleviate reactive power constraints, DC bus voltage constraints, pass band and stop band leading to minimize losses toward improved system efficiency, low temperature loss, and low cost of loss. The LCL filter is designed to suppress harmonics in the inverter output voltage and current so that the smooth voltage and current can be input into the step-up transformer before being injected into the national grid.

The steps for designing the LCL filter are as follows: selecting the switching frequency, selecting the resonance frequency, determining the value of capacitance, and determining the value of inductance. The switching frequency is ten times the resonance frequency, according to some standards. The reactive power supplied by the capacitor at fundamental frequency is used to design the filter capacitor C. In this design, reactive power is set to 5 percent of inverter rated power, grid switching current is set to 0.3 percent of grid current, and grid switching voltage is set to 0.9 times grid voltage[40].

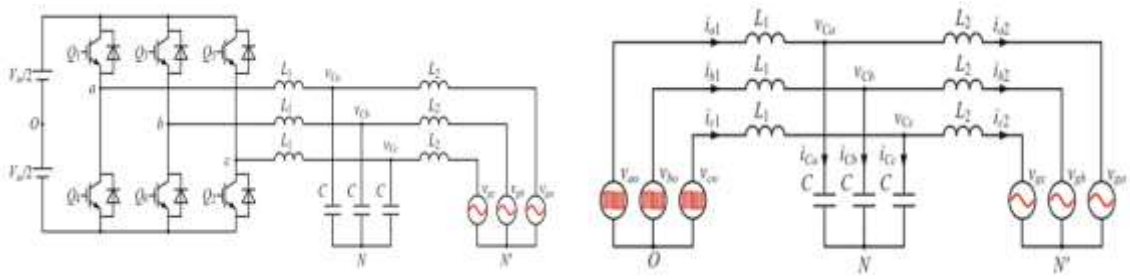

(a) Three phase LCL filter-type Grid connected main circuit

(b) Three phase LCL filter-type Grid connected equivalent circuit

Figure4. 18:Three phase grid connected inverter LCL filter[41]

4.6.3. A complete grid-connected inverter model for FSPV

The modeled part is on the FSPV production side, containing the signal builder for temperature and irradiance as the PV array input. The PV arrays are linked to the boost converter via MPPT incremental conductance, which controls the current and voltage to meet the DC-link voltage connected to the DC-AC converter's input. The inverter's output contains a certain level of harmonics, which is suppressed by the LCL filter. The grid side inductance of the LCL filter suppresses harmonics from the grid. The PLL is yet another component of a grid-connected inverter that synchronizes the voltage, frequency, and phase angle on both sides of the inverter and the grid. As shown in the Fig.4.19, the full model of the grid-connected inverter is created in Matlab software.

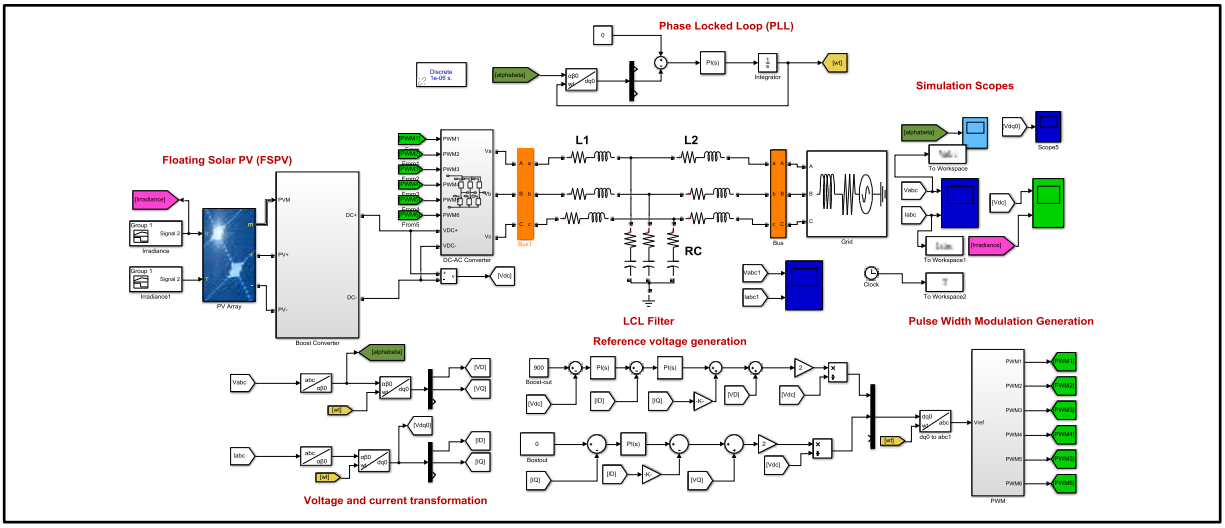

Figure4. 19: Grid connected inverter with LCL filter Matlab model

4.6.4. Grid connected inverter for FSPV power stage

Step-by-step design of an LCL filter for a three-phase grid-connected inverter, as well as the sizing of LCL filter parameters, are provided below.

Grid base impedance:

$$Z_b = {E_n}^2 / P_n \tag{23}$$

Where: E_n is the RMS line to line voltage of the grid.

Base capacitance:

$$C_b = 1/\omega_g Z_b \tag{24}$$

The maximum power factor variation seen by the grid for the filter capacitance is 5%, indicating that the system's phase impedance is adjusted as follows:

$$C_f = 0.05 C_b \tag{25}$$

The base inductance can be deduced from equation:

$$L_b = Z_b / \omega_g \tag{26}$$

And the grid inductance is approximated to be:

$$L_2 = L_{grid} = 0.1 L_b - L_1 \tag{27}$$

The maximum current ripple at the DC-AC inverter's output is given by:

$$\Delta I_{Lmax} = (2V_{dc}/3L_1)(1-m)mT_{sw} \tag{28}$$

It can be seen that at m=0.5, the maximum peak to peak current ripple occurs, and the ripple current becomes:

$$\Delta I_{Lmax} = V_{dc}/6 f_{sw} L_1 \tag{29}$$

Where: L1 is the inverter side inductor

For the design parameters, a 10% ripple of rated current I_{max} is given by:

$$\Delta I_{Lmax} = 0.1 Imax \tag{30}$$

Where: $I_{max} = P_n \sqrt{2}/3V_{ph}$ and Lin becomes: $L_1 = V_{dc}/6 f_{sw} \Delta I_{Lmax}$

The LCL filter should reduce the expected current ripple by 20%, yielding a ripple value of 2% of the output current. Now, harmonic mitigation is given by comparing the harmonic current generated by the inverter to the current injected into the grid:

$$\frac{i_g(h)}{i_i(h)} = \frac{1}{|1 + r[1 - L_{\text{in}} C_b {\omega_{sw}}^2 X]|} = ka \qquad L_2 = \frac{\sqrt{1/{k_a}^2 + 1}}{C_f {\omega_{sw}}^2} \qquad L_2 = rL_1 \tag{31}$$

The constant ka represents the desired attenuation, and r represents the ratio of inductance on the inverter side to that on the grid side. In order to avoid resonance, a resistor in series Rf with the capacitance attenuates some of the ripple on the switching frequency. This resistor's value should be one-third of the filter capacitor's impedance at the resonance frequency.

$$R_f = 1/3\omega_{res} C_f, \qquad \omega_{res} = \sqrt{\frac{L_1 + L_2}{L_1 L_2 C_f}} \tag{32}$$

Where: $10 f_g < f_{res} < 0.5 f_{sw}$

The other parameters considered when designing the LCL filter, is the voltage modulation index and the frequency modulation as the parameters determining the equality of input and output parameters, over-modulation and under-modulation.

Additionally, the care must be taken in selecting the switching frequency as it is proportional to the power loss in the LCL filter. High switching frequency lower the value of filter inductance which is profitable, and a low switching frequency require high value of filter inductance, i.e the power loss in filter reduces as switching frequency is increased. The overall design of the system, switching frequency can be selected to minimize the loss in semiconductor and filter.

Table4.4: Grid connected inverter LCL filter design parameters

Design parameters	Values	Units
Inverter output voltage frequency(f)	50	Hertz (Hz)
Filter inverter side inductance(L1)	7e-3	Henry (H)
Filter grid side inductance (L2)	7e-7	Henry (H)
Filter capacitance(C)	3e-3	Farad (F)
Filter damping resistor (R)	7e-3	Ohm (Ω)

4.6.5. Grid connected inverter for FSPV simulation

The grid-connected inverter serves as a link between the FSPV and the grid. The closed loop or control of the grid-connected inverter allows the inverter output voltage, frequency, and phase angle to be synchronized with the grid. Fig.4.19 (a) depicts the inverter's output voltage before the insertion of an LCL filter and Fig. 4.19(b) depicts the voltage and the current after inserting the filter. The voltage at the inverter's output after the filter is always constant, and obtaining maximum values in simulation is $400 * \sqrt{2}$ which 565.68 Volt (peak to peak).

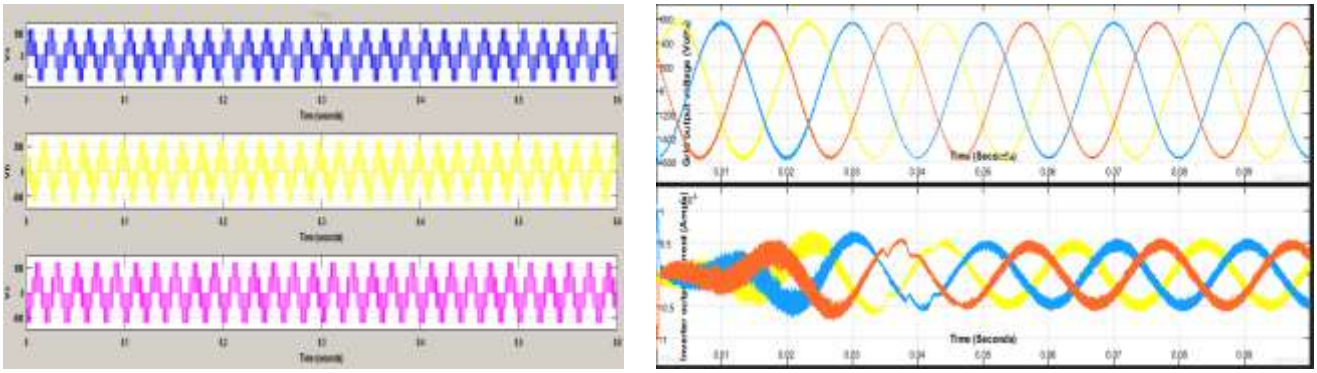

(a) (b)

Figure4. 20: Grid connected inverter voltage: (a) Phase to phase voltage and (b) Current waveforms before and after inserting LCL filter

During switching time, the THD was high compared to the THD after 0.05 sec. The total harmonics distortion at t=0.05sec from switching was significantly reduced towards the stability of the system as indicated in Fig.4.23 and Fig.4.24. THD for inverter output voltage was found to be 0.053%, while THD for inverter output current was 1.56% which are within IEEE (519-2014) standards.

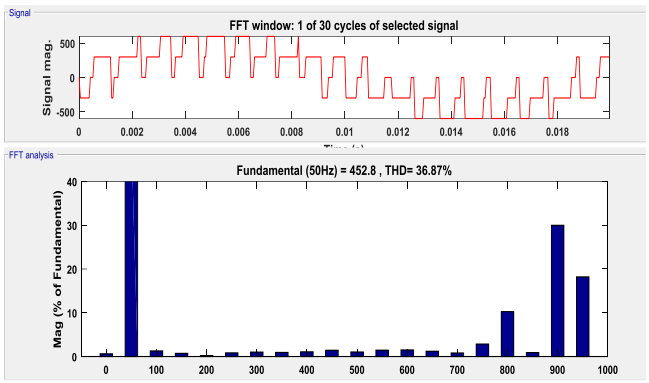

Phase voltage a

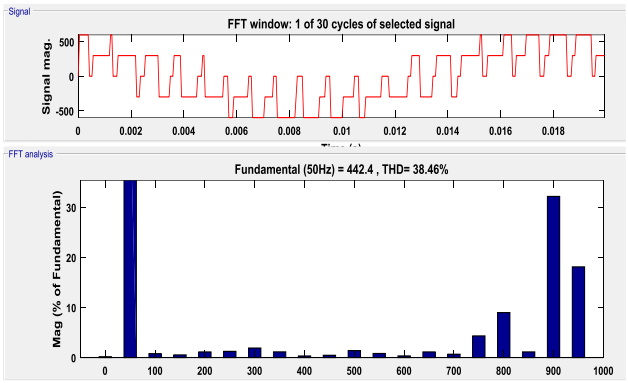

Phase voltage b

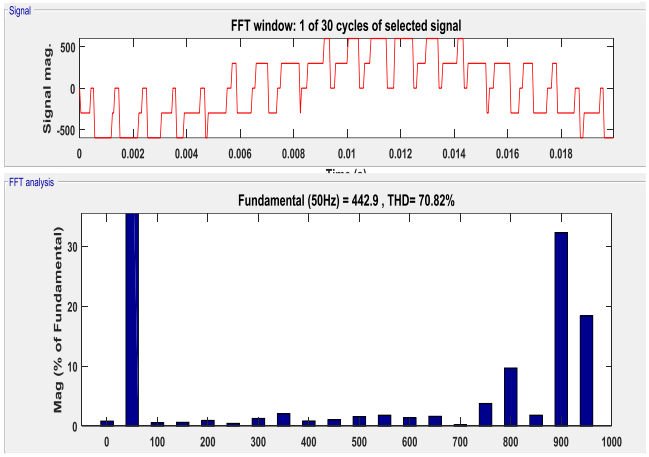

Phase voltage c

Phase voltage	THD
Phase a	36.87%
Phase b	38.46%
Phase c	70.82%

Phase voltage THD percentage

Figure4. 21: Inverter output voltage THD distortion before inserting the filter (Va, Vb, Vc)

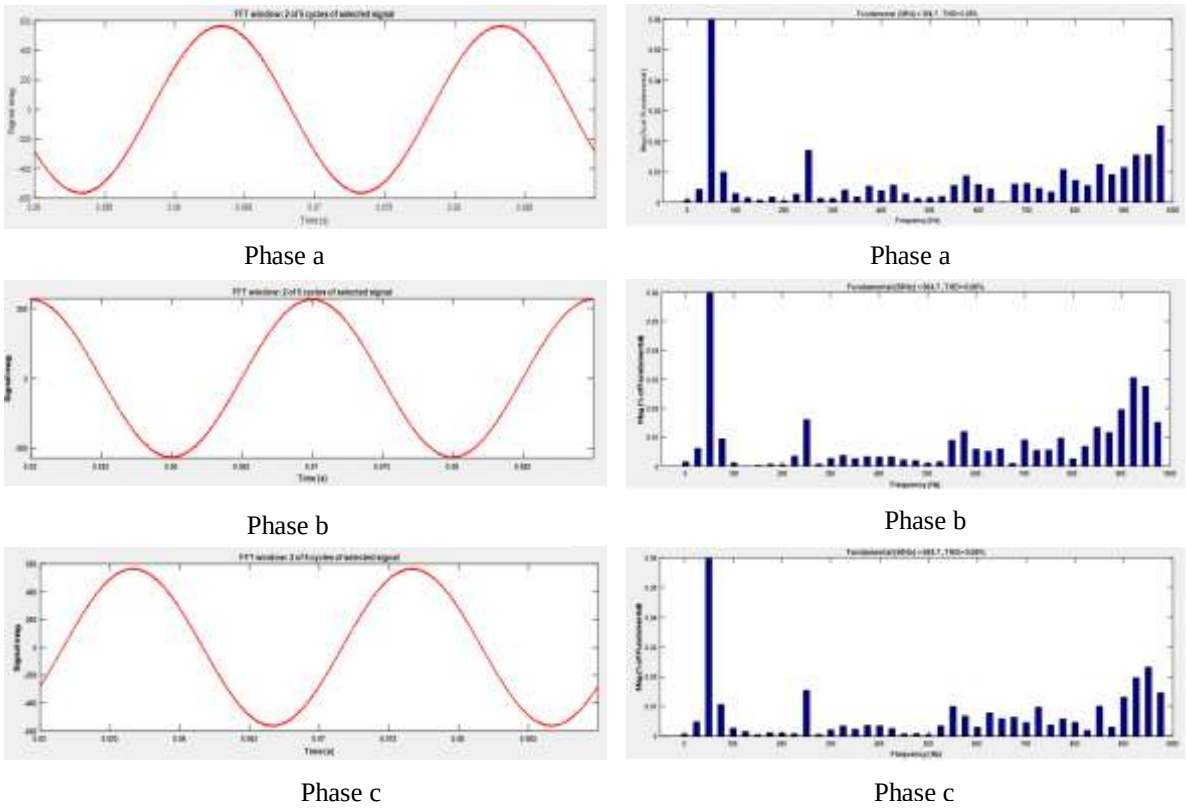

Figure4. 22: Grid connected inverter output voltage after inserting LCL filter THD at t=0.05secs

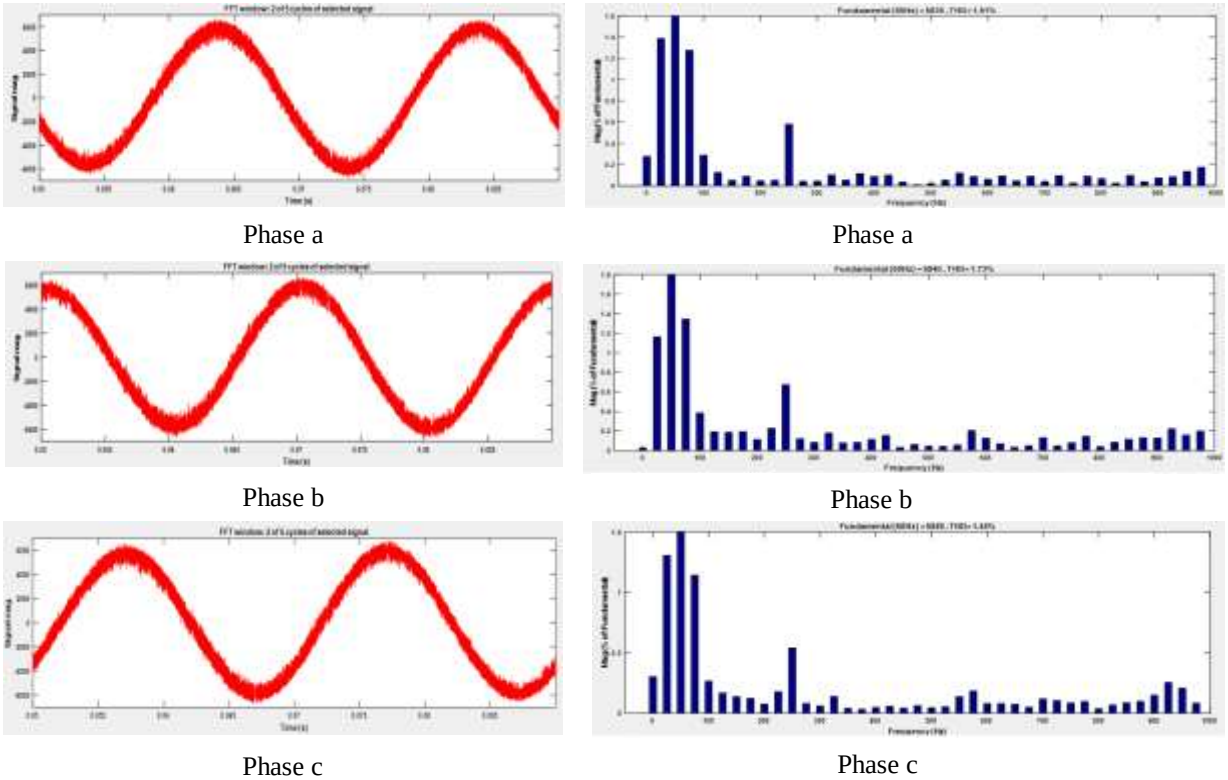

Figure4. 23: Grid connected inverter output current after inserting LCL filter THD at t=0.05secs

CHAPTER V: RESULTS AND DISCUSSIONS

5.0. Introduction

This chapter highlights the study's findings, which realize the study's objectives of designing the FSPV, modeling, and simulation, its contribution to land management, its contribution to moving from traditional SPV systems to other alternative FSPV technologies, GHGS reduction, water body quality improvement, and maximizing the use of existing HPP infrastructures. For data analysis, PVsyst, Matlab, and Microsoft Excel were used.

The Sunpower-SPR-445NJ-WHTD.PAN, Si-mono-crystalline PV module, with sub-array of 675 parallel strings and 10 series modules, the closed loop boost converter, and the closed loop inverter are used to complete the system design. The design was done referring to available water body, shadow consideration, the load profile of Nyabarongo HPP and meteorological data at the place as well. The impact of FSPV on the grid was analyzed through harmonics analysis. The temperature, irradiance, and wind speed of the site are other parameter used to show that the FSPV is more efficient compared to land based SPV.

5.1. Load profile of Nyabarongo HPP

The previous chapters demonstrate the FSPV's good performance; however, the load profile of Nyabarongo must be considered before discussing the FSPV's interconnection to the existing system. The July 2021 load profile for Nyabarongo HPP is shown in Fig.5.1, which shows the power delivered by each of the two generating units at Nyabarongo HPP over a given time period. When both generating units are operational at the same time, they deliver 28 MW of power to the grid. Where each generator generates 14 MW at its maximum. The load profile presented in Fig.5.1, it is only for the month of July/2021.

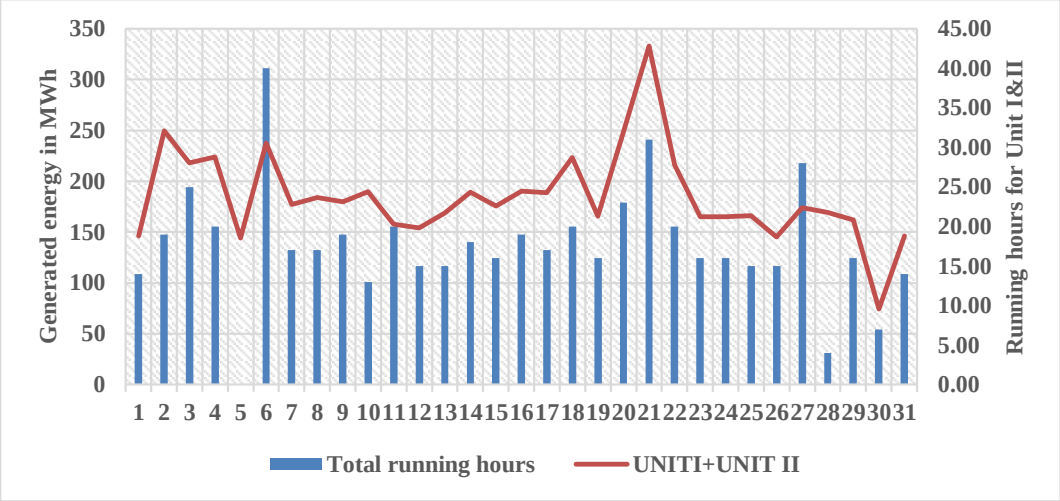

Figure5. 1: Nyabarongo HPP July/2021 load profile

Total running hours in July/2021 for generating unit I and II are 545 hours, in these hours the generated energy was 5,729.2 MWhrs, the minimum energy generated energy was 74.3 MWhrs on 30th July/2021, while the maximum energy generated was 333 MWhrs within 31 hours on 21st July/2021. The FSPV comes in support during the day, in sunny period, to inject the power of 28 MW, for single unit with FSPV farm. In the case where both units are in operation, the FSPV and Nyabarongo HPP units inject together into the grid 42 MW at time. During the night, FSPV is not in operation, only the hydro power plant which must inject 28 MW for two units in operation or 14MW for one unit. To meet the demand of 42 MW during the night, it is required to incorporate storage to support the HPP.

5.2. FSPV potential energy contribution

The potential energy production of the FSPV is shown in Fig.5.2, where the energy produced was 2,234,123 kWh, and the energy injected into the grid was 2,198,176 kWh, indicating a 98.4 percent efficiency of the FSPV. According to the PVsyst software simulation, the average output energy of the grid-connected inverter is 24,088,671.0 kWh, and the average efficiency of the inverter is 98.4 percent, as shown in the Fig.5.3.

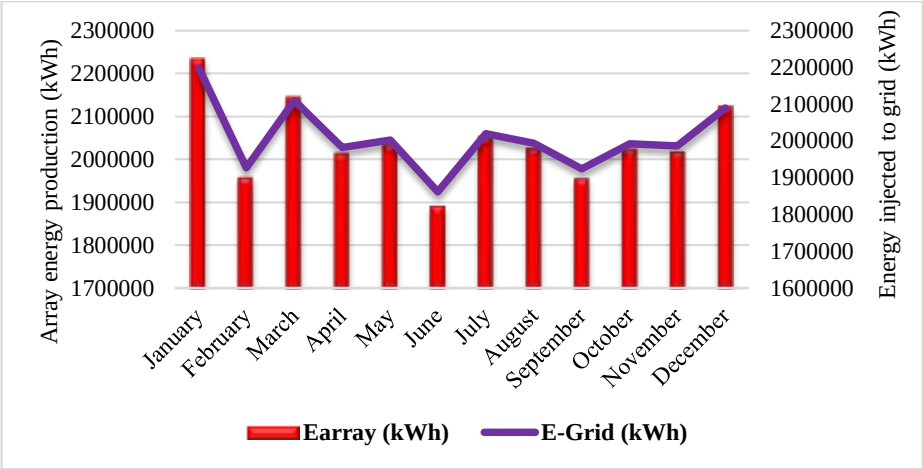

Figure5. 2: Array produced energy and injected energy into the grid

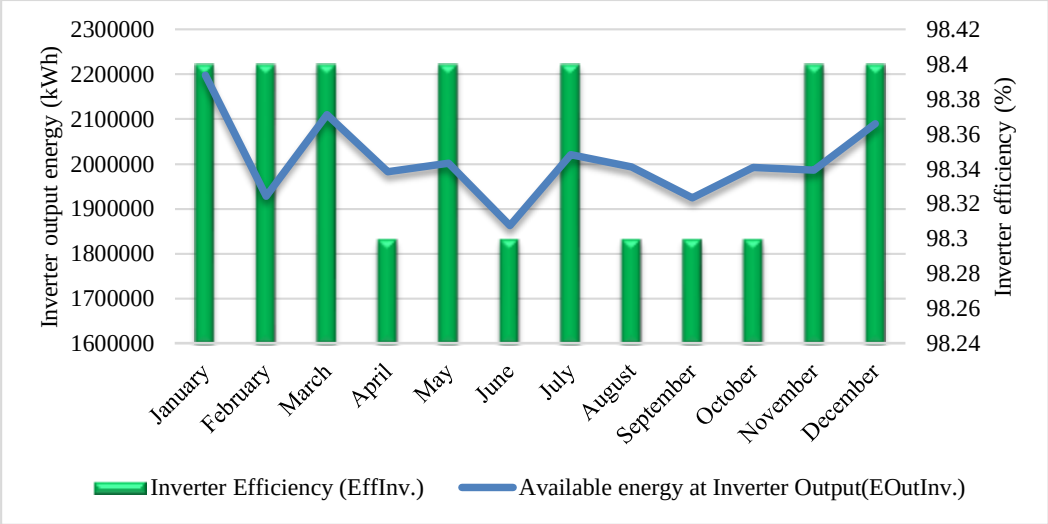

Figure5. 3: Grid connected inverter output energy and its efficiency

The Fig.5.4 presents that the inverter global average loss was found to be 35,197.75 kWh, the average array mismatch loss was 44,279.58 kWh, and the average loss due to electrical shading was 397.47 kWh.

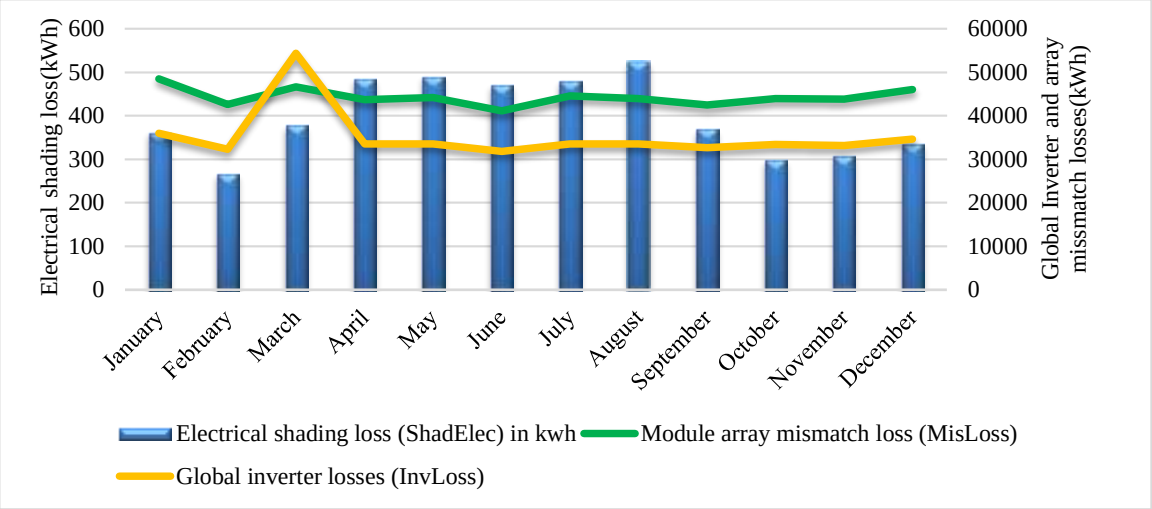

Figure5. 4: Shading loss, Inverter global loss, and array loss

5.3. Contribution of the FSPV

From the PVsyst software analysis of FSPV potential energy production, the FSPV in each month from January to December the maximum energy produced is found in January where 2,234,123 kWh are produced, the minimum production is found in June, where 1,893,845 kWh are produced. The maximum performance ratio is found in May of 82% and minimum of 80.7% is found in February. Usually, Nyabarongo HPP deliver 14 MW for single generating unit or 28 MW for two generating units. After integrating with FSPV, both deliver to the grid 42 MW during the day, and in sunny period to satisfy the increasing load demand of today. If the demand is only 28 MW, a single generating unit with FSPV inject in the grid 28 MW, and during this time water in dam will be stored for running two units during the night when the demand is 28 MW. As FSPV is integrated with HPP, the capacity factor of the hydro power plant increases. The hydropower plant dam water surface that has not been exploited is being used for this FSPV project to maximize the use of Nyabarongo infrastructures.

The FSPV contributes to land use management specifically because it only uses water bodies such as reservoirs, hydroelectric dams, industrial ponds, irrigation ponds, reservoir, water treatment ponds, mining ponds, wastewater treatment plants, wineries, fish farms, canals, lakes, oceans, and lagoons. Traditional solar PV systems require a large surface of land, which could be used for agriculture or other purposes. To solve this agriculture conflicts with traditional solar PV, FSPV technologies are used.

The FSPV design on the selected site, inject an amount of 15 MW, this compensate the load demand which exponentially increasing today. Today, as the fossil fuels are the source of GHGs, which harm the environment, in these centuries, the use of FSPV, minimize significantly this emission of GHGs. Furthermore, because the efficiency of solar energy is affected by temperature, and the FSPV installed

on water bodies has self-cooling, it ensures high efficiency when compared to land-mounted solar PV, so the FSPV technology is used instead of the traditional means.

Many dams and hydropower plants in Rwanda are underutilized due to the lack of use of this new solar energy generation technology; in order to maximize the use of existing hydropower plant infrastructures, this technology must be adopted. The potential production of the FSPV demonstrated that in Rwanda, if the available water resources surfaces are used for energy production, the target in energy access from a rate 51% (37 on-grid and 14 % off-grid) to 52% on grid and 48% off-grid by 2024 with a capacity of 556 MW can be achieved easily by installing the FSPV on water body surfaces not currently in use. As the ambient temperature on Nyabarongo HPP dam is 19.8^{o} C, and the global horizontal irradiance of 5.83 kWh/m^2, this ensure high efficiency in energy generation compared to ground mounted solar PV that has less efficiency due to their cooling difficulties. The potential power of Nyabarongo HPP dam is beyond the extracted small area providing 15 MWp as simulated by the use of PVsyst software. The system production was 24,087 MWh/year, specific production of 1,064 kW/kWp/year, the performance ratio of 82% and system losses of 0.07kW/kWp/day, the normalized production of the FSPV has been shown as 4.39 kW/kWp/day.

5.3. FSPV Three phase inverter harmonics analysis

The interaction of the FSPV must adhere to the existing network's standards. As a result, the level of harmonics must be discussed. The following are the primary design goals of closed loop current control for the FSPV grid-connected inverter: (1) a small steady-state error in grid current; (2) a fast dynamic response with low overshoot; and (3) a low inverter THD. The Fast Fourier transform (FFT) analysis of inverter output current and voltage THD was found to be within IEEE (519-2014) standards for 69 kV to 161 kV, which is 2.5 percent for voltage and 3 percent for current. The Table5.1 and 5.2 show the level of harmonics on the output voltage and current of the FSPV inverter.

Table5. 1: THD measured in the AC side phase voltages of the inverter (fundamental frequency 50Hz)

Phase voltage	THD (at t=0sec)	THD (at t=0.05sec)
Va	0.68%	0.05%
Vb	1.47%	0.06%
Vc	0.88%	0.05%

Table5. 2: THD measured in the AC side phase currents of the inverter (fundamental frequency 50Hz)

Phase current	THD (at t=0sec)	THD (at t=0.05sec)
Ia	49.36%	1.51%
Ib	74.71%	1.73%
Ic	63.52%	1.44%

5.4. Comparison of FSPV at different sites with FSPV at Nyabarongo site

The results in chapter 4 proved that the Nyabarongo HPP dam is potential for the FSPV. Yet, a comparison with other sites is necessary to be sure that the FSPV is not only feasible at Nyabarongo site but also it can be applied on other sites. The FSPV is feasible in Rwanda because water bodies such as Nyabarongo HPP dam, Rusizi HPP dam, Mukungwa HPP dam, Ntaruka HPP dam, and others sites are available, as well as lakes such as Cyohoha lake, Rweru lake, Birara lake, Sake lake, Mugesera lake, Rwanyakizinga lake, Muhindi lake, Hago lake, Kivumba lake, Ihema lake, Rwakibali. The average irradiance on the lakes listed is 5.7kW/m^2/day, which is adequate for any solar PV system. The ambient temperature on the available lakes is discovered to be less than the STC temperature of 25^{o}C. As the land mounted SPV cooling capability is low, the operating temperature of the traditional SPV is high compared to the FSPV as indicated in Fig.5.5, and Fig.5.6.

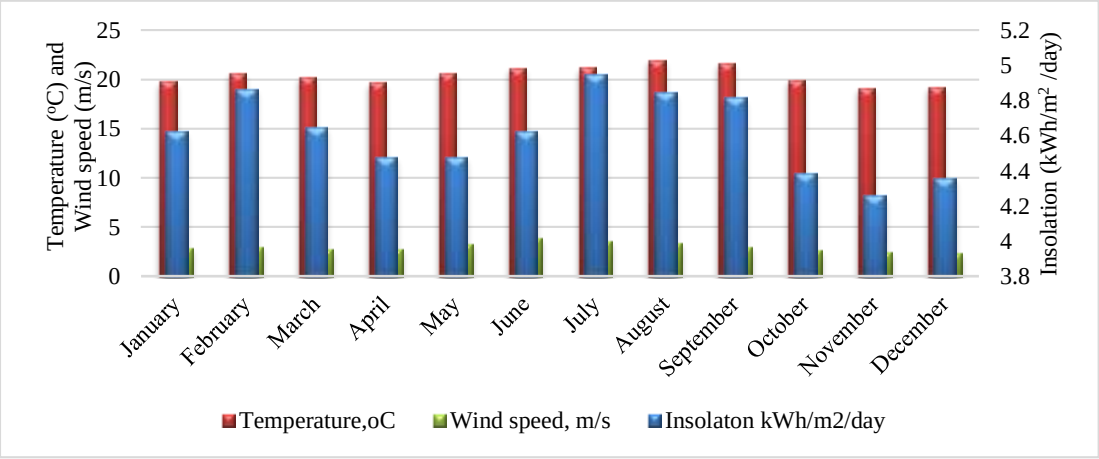

Figure5.5: Rwamagana GigaWatt meteorological data

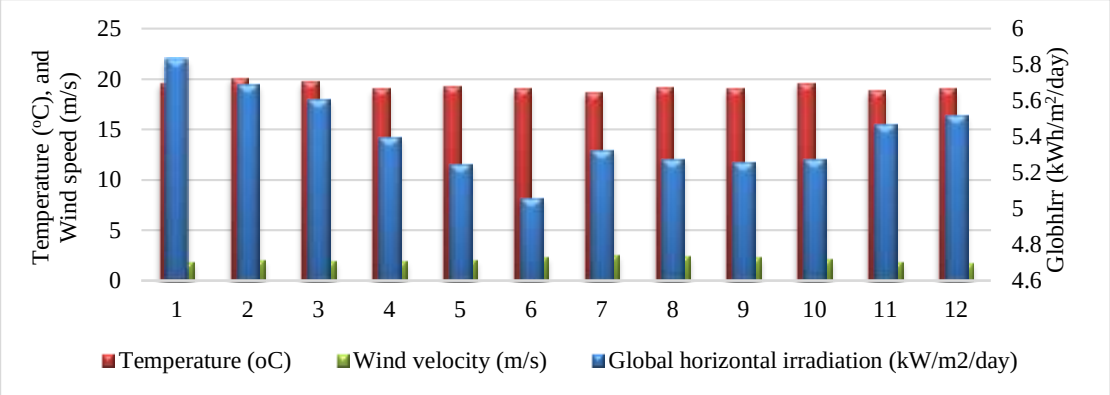

Figure5. 5: Nyabarongo HPP dam meteorological data

As the ambient temperature is the key factor determining the efficiency of the FSPV system, the Fig. 5.7., shows the temperatures of the five lakes i.e; Lake Ihema, Lake Mugesera, Lake Rweru, Lake Birara, and Lake Burera. Their temeperatures are under the STC temperature 25°C which predict the feasibility of FSPV installation in Rwanda.

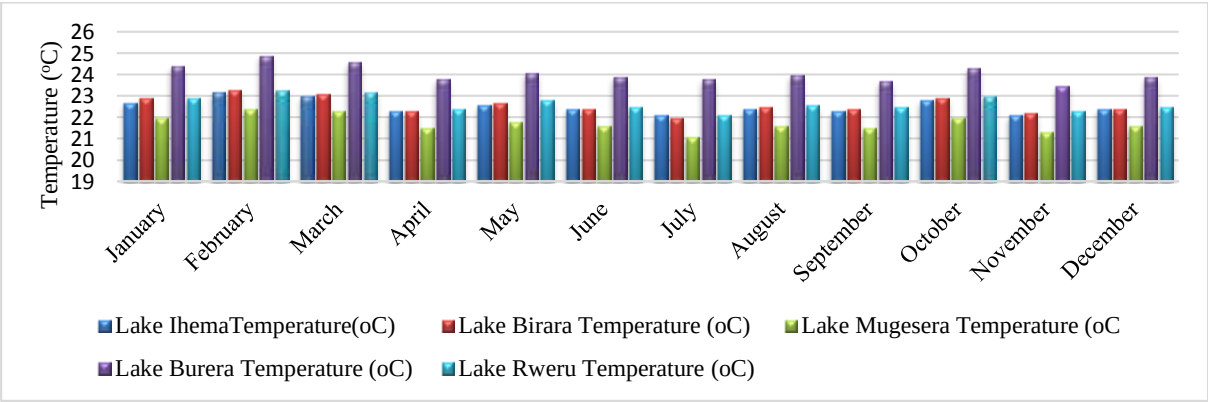

Figure5. 6: Temperature of some Lakes in Rwanda (Meteo data)

Fig.5.8, shows the temperatures and global irradiance of the five selected lakes showing that the FSPV is feasible as temperature and irradiances are within allowable values.

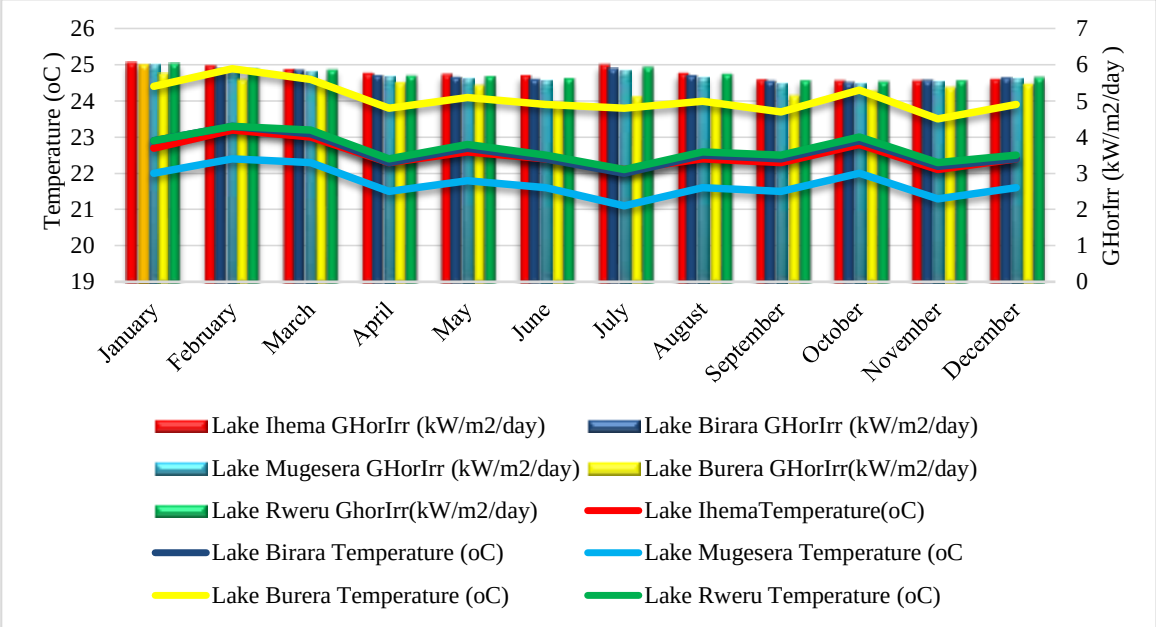

Figure5. 7: Temperature and global horizontal irradiance of some Lakes in Rwanda

5.5. FSPV integration with HPP

The integration of this FSPV is exciting because the goal is to maximize the utilization of existing infrastructure to avoid the additional costs associated with transmission and distribution of generated power. Although there are various methods of power transmission, the existing transmission lines of 110kV are used to keep the research goal of minimizing costs. Because it is the closest substation to the FSPV power plant, the Nyabarongo HPP sub-station is used. To connect the FSPV to the 110kV grid, the low voltage of 400V from the inverter's output is stepped up with a transformer rated 400/6.6kV and then to the substation transformer rated 6.6/110kV. The minimum investment will be ready to be use once the FSPV connection is established. The capacity factor of the existing HPP is also improved.

CHAPTER VI: CONCLUSION AND RECOMMENDATIONS

6.0. Introduction

This chapter provides a summary, conclusion, recommendation, and areas for future research on topics related to **''Design of floating solar photovoltaic system integrated with a hydropower plant (a case study Nyabarongo HPP dam)''.** Recommendations are addressed to all Rwandan energy stakeholders: policy makers, regulators, companies' suppliers, investors, households' members, and readers to achieve sustainably the universal energy access by 2024. A technical feasibility of FSPV at the site was done towards the international standards, such as nominal power ratio, performance ratio, and total harmonics distortion percentage for inverter output voltage and the current. The questions which formed the basis of this thesis work are presented here again:

What is the improvement in photovoltaic energy generation efficiency, if the traditional SPV system is replaced by floating solar photovoltaic system?

Does floating solar PV contribute to optimal use of existing HPP infrastructures?

6.1. Conclusion

The goal of this study was to design the FSPV on the Nyabarongo HPP dam, evaluate its technical feasibility, and assess its impact on the grid. To achieve the designed system's stability, a DC-DC converter was used to boost the output voltage of the PV array and perform MPPT using the IC technique. In the d-q reference frame, a three phase-two level VSI was controlled to inject the maximum active power into the grid. The PVsyst software was used to simulate the potential electrical energy generated by FSPV. To validate the performance of the proposed system, computer simulation was performed using the MATLAB/Simulink software environment. The simulation results show that the control techniques provide an excellent steady-state response with low steady-state error, a fast dynamic response, a low total harmonic current distortion, and high quality injected current into the grid. Furthermore, the current controller aligns the current injected into the grid with the grid voltage. The FFT analysis of the inverter output current demonstrates that the THD is within acceptable limits. This ensures that the power output of the Nyabarongo HPP is maximized and the FSPV energy injection into the grid is of high quality. The findings of this study project a good use of existing infrastructure and an increase in the capacity factor of the Nyabarongo HPP. The installation of FSPVs on available water bodies in Rwanda anticipates meeting the increasing load demand day by day, as well as GHGS because it is a renewable energy source. The FSPV installation increases energy generation capacity due to its ease of cooling; however, in order to improve efficiency and land use management, some existing ground

mounted SPV can be replaced with installation of FSPV where it is possible for managing the land resource. As previously stated, the implementation of innovative technologies such as floating solar PV power plants is a reasonable step toward achieving 100 percent access to electricity by 2024.

6.2. Recommendations

This study's recommendations emphasize four points: policy framework, policymakers, energy developers, energy regulators, researchers, and renewable energy developer companies:

- Implementing the renewable energy policy framework as target of increasing the renewable energy in the energy mix, will stimulate the involvement of individual players, and local players in the energy sector by providing to them necessary infrastructure to motivate the development, encourage the banks and other private sectors to be involved in the achievement of the universal energy access to reliable, affordable, and sustainable energy development.
- Through renewable energy policy makers, the emission and climate change effect will be reduced by elaborating policies encouraging the energy developers to move from the traditional means which emit GHGS as source of air pollution, to the new technology of energy generation from the use of renewable resources such as FSPV, hydro-energy, and agro-photovoltaic towards the sustainable energy development, and meet the increasing load demand of today.
- The Ministry of Education has to invest more in renewable energy research development, and establish more renewable energy centers to empower the research in this field towards smart grid of the future.
- To successfully implementation of this new technology and other renewable energy alternatives, more effort must be put in awareness campaign to motivate internal young entrepreneurs and external companies working on the renewable energy development.
- As local SPV companies are competing for land including agriculture, industries and population growth due to lack of space and space limitations, it is recommended to MININFRA to put more effort to exploit the available water bodies in Rwanda as our country is among countries with weak land electrical network.

6.3. Area of further research

This study was limited on FSPV with temperature and irradiance variations under control. The voltage and current control of a grid-connected inverter were controlled, further research will be conducted on three highlighted points.

1. Grid connected FSPV load variation control (frequency control)
2. The impact of FSPV on Nyabarongo HPP dam biodiversities,
3. Economic feasibility of FSPV on Nyabarongo HPP dam and GHGS emission
4. Techno-economic feasibility of FSPV on Nyabarongo HPP dam

REFERENCES

[1] E. Hakizimana, A. Ngendahayo, U. G. Wali, D. Sandoval, and V. Kayibanda, "Analysis of Environmental Impacts of Solar Energy Technologies in Rwanda: GigaWatt," *Energy Environ. Eng.*, vol. 7, no. 2, pp. 38–49, 2020, doi: 10.13189/eee.2020.070203.

[2] H. Liu, V. Krishna, J. L. Leung, T. Reindl, and L. Zhao, "Field experience and performance analysis of floating PV technologies in the tropics," no. April, pp. 1–11, 2018, doi: 10.1002/pip.3039.

[3] J. Suh, Y. Jang, and Y. Choi, "Comparison of electric power output observed and estimated from floating photovoltaic systems: A case study on the hapcheon dam, Korea," *Sustain.*, vol. 12, no. 1, 2020, doi: 10.3390/su12010276.

[4] G. Bamundekere, "Contributions of Renewable Energy to Sustainable Development in Africa: Case Study of Solar Energy in Rwanda," no. July 2019, 2019.

[5] A. Edward, "Mounting Your Solar Photovoltaic (PV) System Mounting Your Solar Photovoltaic (PV) System," no. May, 2020.

[6] "I&M Bank Headquarters." http://www.bettstownsend.com/Projects/I%26M-Bank-Headquarters (accessed Sep. 04, 2021).

[7] "BIPV with huge potential for greener cities - pv Europe." https://www.pveurope.eu/solar-generator/bipv-huge-potential-greener-cities (accessed Sep. 04, 2021).

[8] "Building Integrated Photovoltaics : A Concise Description of the Current State of the Art and Possible Research Pathways," pp. 1–30, 2016, doi: 10.3390/en9010021.

[9] P. C. Treaty, *The Floating PV Plant 1*. 2018.

[10] E. Kjellsson, "Potential for building integrated photovoltaics," *IEA-PVPS Task*, vol. 2002, p. 4, 2002, [Online]. Available: http://scholar.google.com/scholar?hl=en&btnG=Search&q=intitle:POTENTIAL+FOR+BUILDING+INTEGRATED+PHOTOVOLTAICS#4%5Cnhttp://ptp.irb.hr/upload/mape/solari/31_Elisabeth_Kjellsson_Potential_for_Building_Integrated_Phot.pdf.

[11] A. B. Awan, M. Alghassab, M. Zubair, A. R. Bhatti, M. Uzair, and G. Abbas, "Comparative analysis of ground-mounted vs. rooftop photovoltaic systems optimized for interrow distance between parallel arrays," *Energies*, vol. 13, no. 14, 2020, doi: 10.3390/en13143639.

[12] R. Cazzaniga and M. Rosa-Clot, "The booming of floating PV," *Sol. Energy*, no. June, 2020, doi: 10.1016/j.solener.2020.09.057.

[13] R. Cazzaniga, M. Rosa-Clot, P. Rosa-Clot, and G. M. Tina, "Integration of PV floating with

hydroelectric power plants," *Heliyon*, vol. 5, no. 6, p. e01918, 2019, doi: 10.1016/j.heliyon.2019.e01918.

[14] B. Z. Taye, A. H. Nebey, and T. G. Workineh, "Design of floating solar PV system for typical household on Debre Mariam Island Design of floating solar PV system for typical household on Debre Mariam Island," 2020, doi: 10.1080/23311916.2020.1829275.

[15] "Where Sun Meets Water," *Where Sun Meets Water*, 2019, doi: 10.1596/32804.

[16] N. Lee *et al.*, "Hybrid floating solar photovoltaics-hydropower systems: Benefits and global assessment of technical potential," *Renew. Energy*, vol. 162, pp. 1415–1427, 2020, doi: 10.1016/j.renene.2020.08.080.

[17] E. Solomin, E. Sirotkin, E. Cuce, S. P. Selvanathan, and S. Kumarasamy, "Hybrid Floating Solar Plant Designs: A Review," *Energies*, vol. 14, no. 10, p. 2751, 2021, doi: 10.3390/en14102751.

[18] M. Acharya and S. Devraj, "Floating Solar Photovoltaic (FSPV): A Third Pillar to Solar PV Sector," *Energy Resour. Institute. Available https//www. teriin. org/sites/default/files/2020-01/floating-solar-PV-report. pdf (Accessed 3 May 2020)*, 2019.

[19] S. K, "SWOT analysis of floating solar plants," *MOJ Sol. Photoenergy Syst.*, vol. 3, no. 1, pp. 20–22, 2019, doi: 10.15406/mojsp.2019.03.00030.

[20] A. K. Tripathi and C. S. N. Murthy, "Effect of shading on PV panel technology," *2017 Int. Conf. Energy, Commun. Data Anal. Soft Comput. ICECDS 2017*, pp. 2075–2078, 2018, doi: 10.1109/ICECDS.2017.8389814.

[21] M. M. Fouad, L. A. Shihata, and E. S. I. Morgan, "An integrated review of factors influencing the performance of photovoltaic panels," *Renew. Sustain. Energy Rev.*, vol. 80, no. June, pp. 1499–1511, 2017, doi: 10.1016/j.rser.2017.05.141.

[22] C. Saiprakash, A. Mohapatra, B. Nayak, and S. R. Ghatak, "Analysis of partial shading effect on energy output of different solar PV array configurations," *Mater. Today Proc.*, vol. 39, no. xxxx, pp. 1905–1909, 2021, doi: 10.1016/j.matpr.2020.08.307.

[23] *The Performance of Photovoltaic (PV) Systems*. 2017.

[24] S. Gallardo-Saavedra and B. Karlsson, "Simulation, validation and analysis of shading effects on a PV system," *Sol. Energy*, vol. 170, no. June, pp. 828–839, 2018, doi: 10.1016/j.solener.2018.06.035.

[25] B. Pakkiraiah and G. D. Sukumar, "Research Survey on Various MPPT Performance Issues to Improve the Solar PV System Efficiency," *J. Sol. Energy*, vol. 2016, pp. 1–20, 2016, doi:

10.1155/2016/8012432.

[26] M. C. Argyrou and C. C. Marouchos, “A Grid-connected Photovoltaic System : Mathematical Modeling using MATLAB / Simulink,” 2017.

[27] M. Hlaili and H. Mechergui, “Comparison of Different MPPT Algorithms with a Proposed One Using a Power Estimator for Grid Connected PV Systems,” *Int. J. Photoenergy*, vol. 2016, 2016, doi: 10.1155/2016/1728398.

[28] A. Safari and S. Mekhilef, “Incremental conductance MPPT method for PV systems,” *Can. Conf. Electr. Comput. Eng.*, pp. 000345–000347, 2011, doi: 10.1109/CCECE.2011.6030470.

[29] N. Hussein Selman, “Comparison Between Perturb & Observe, Incremental Conductance and Fuzzy Logic MPPT Techniques at Different Weather Conditions,” *Int. J. Innov. Res. Sci. Eng. Technol.*, vol. 5, no. 7, pp. 12556–12569, 2016, doi: 10.15680/ijirset.2016.0507069.

[30] A. Yahfdhou, A. Mahmoud, and I. Youm, “Modeling and optimization of a photovoltaic generator with matlab/simulink,” *Int. J. I Tech E Eng.*, vol. 3, no. 4, pp. 108–111, 2013.

[31] N. D. Kaushika, A. Mishra, and A. K. Rai, *Solar Photovoltaics*. .

[32] M. G. U. I. Environment, I. H. Altas, and A. M. Sharaf, “A Photovoltaic Array Simulation Model for,” no. 1, pp. 341–345.

[33] H. M. Q. M. A. J. Y. E.-C. Y. H. J. Yousuf, “A Review on Floating Photovoltaic Technology (FPVT),” *Curr. Photovolt. Res.*, vol. 8, no. 3, pp. 67–78, 2020, [Online]. Available: https://doi.org/10.21218/CPR.2020.8.3.067.

[34] M. O. F. Environment, “REPUBLIC OF RWANDA MINISTRY OF ENVIRONMENT,” 2018.

[35] R. A. Shaffer, *Fundamentals of power electronics with MATLAB*. Firewall Media, 2013.

[36] “ECEN2060 MATLAB/Simulink materials.” http://ecee.colorado.edu/~ecen2060/matlab.html (accessed Jul. 13, 2021).

[37] F. Ayadi, I. Colak, N. Genc, and H. I. Bulbul, “Impacts of wind speed and humidity on the performance of photovoltaic module,” *8th Int. Conf. Renew. Energy Res. Appl. ICRERA 2019*, pp. 229–233, 2019, doi: 10.1109/ICRERA47325.2019.8996718.

[38] A. Vangari and J. N. Sakamuri, “Dynamics of Voltage Source Converter in a Grid Connected Solar Photovoltaic System,” no. July, 2015, doi: 10.1109/IIC.2015.7150768.

[39] “(7) Simulation of 3 phase grid connected inverter using MATLAB with dq Control. - YouTube.” https://www.youtube.com/watch?v=US3tsnUOJL0&t=1734s (accessed Oct. 03, 2021).

[40] F. Liu, X. Zha, and S. Duan, “Design and research on parameter of LCL filter in three-phase

grid-connected inverter," *Diangong Jishu Xuebao/Transactions China Electrotech. Soc.*, vol. 25, no. 3, pp. 110–116, 2010.

[41] X. Ruan, X. Wang Donghua Pan, D. Yang Weiwei Li, and C. Bao, *Control Techniques for LCL-Type Grid-Connected Inverters*. 2018.

APPENDICES

Appendix 1: Nyabarongo HPP Dam

Appendix 2: Nyabarongo HPP substataion

Appendix 3: Nyabarongo HPP Power House

Appendix 4: Incremental Conductance mppt Matlab Codes

```
function y = MPPT_InC(V_PV,I_PV,Vo, Io, D)
m=0;
dV=V_PV-Vo;
dI=I_PV-Io;
if dV==0
if dI==0
    m=D;
else
    if dI>0
        m=D-0.0001;
    else
        m=D+0.0001;
    end
end
elseif dI/dV==-(I_PV/V_PV)
else
    if dI/dV>-(I_PV/V_PV), m=D-0.001;
    else
       m=D+0.0001;
    end
end
y=m;
end
```

Appendix 5: Some important formulae used for grid connected inverter:

Efficiency of the inverter: $\eta_{Inv} = \frac{P_{Out}}{P_{In}} \times 100 = \frac{P_{ac}}{P_{dc}} \times 100$

European Inverter efficiency:

$$\eta_{Inv(EUR)} = 0.03\eta_{5\%} + 0.06\eta_{10\%} + 0.13\eta_{20\%} + 0.10\eta_{30\%} + 0.48\eta_{50\%} + 0.2\eta_{100\%}$$

Carfornia Energy Commission Inverter efficiency:

$$\eta_{Inv(CEC)} = 0.04\eta_{10\%} + 0.05\eta_{20\%} + 0.12\eta_{30\%} + 0.21\eta_{50\%} + 0.53\eta_{75\%} + 0.05\eta_{100\%}$$

Efficiency of the PV module: $\eta_{PV} = \frac{P_{MPP}}{G \times A}$

Performance Ratio of PV system: $PR = \frac{E}{G \times A \times \eta}$

Total efficiency of the PV system: $\eta_{Tot} = \eta_{module} \times PR$

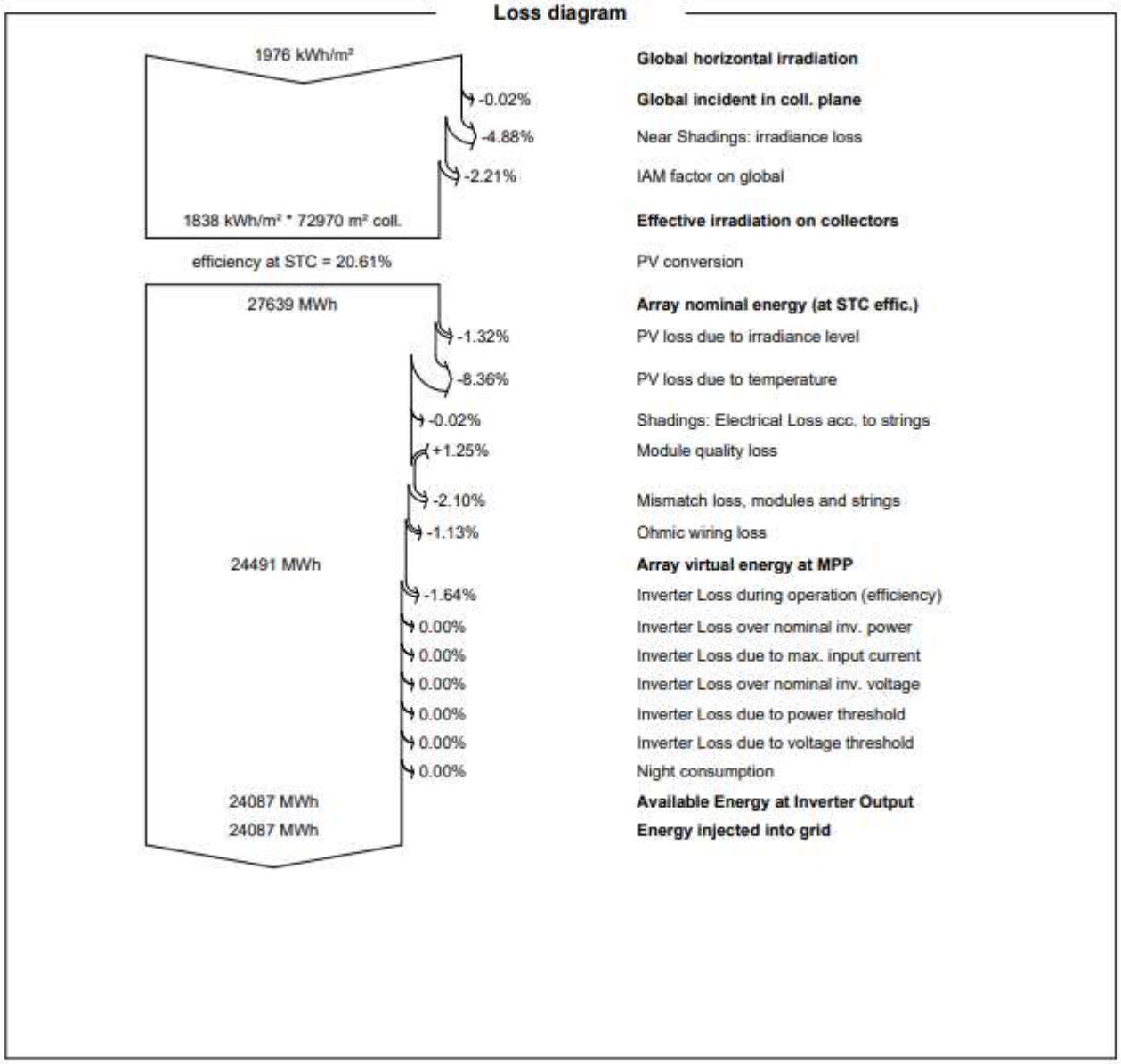

Appendix 6: PV system loss diagram in PVsyst software

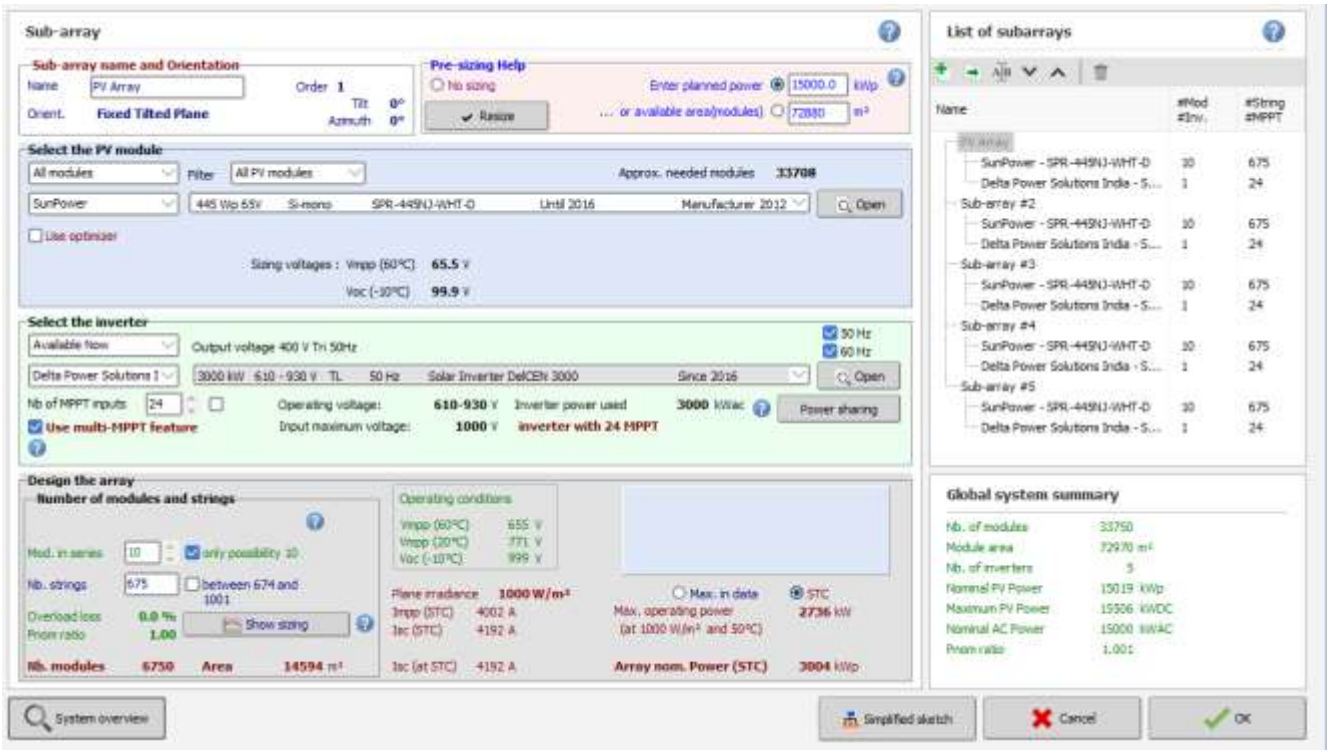

Appendix 7: System overview in PVsyst software

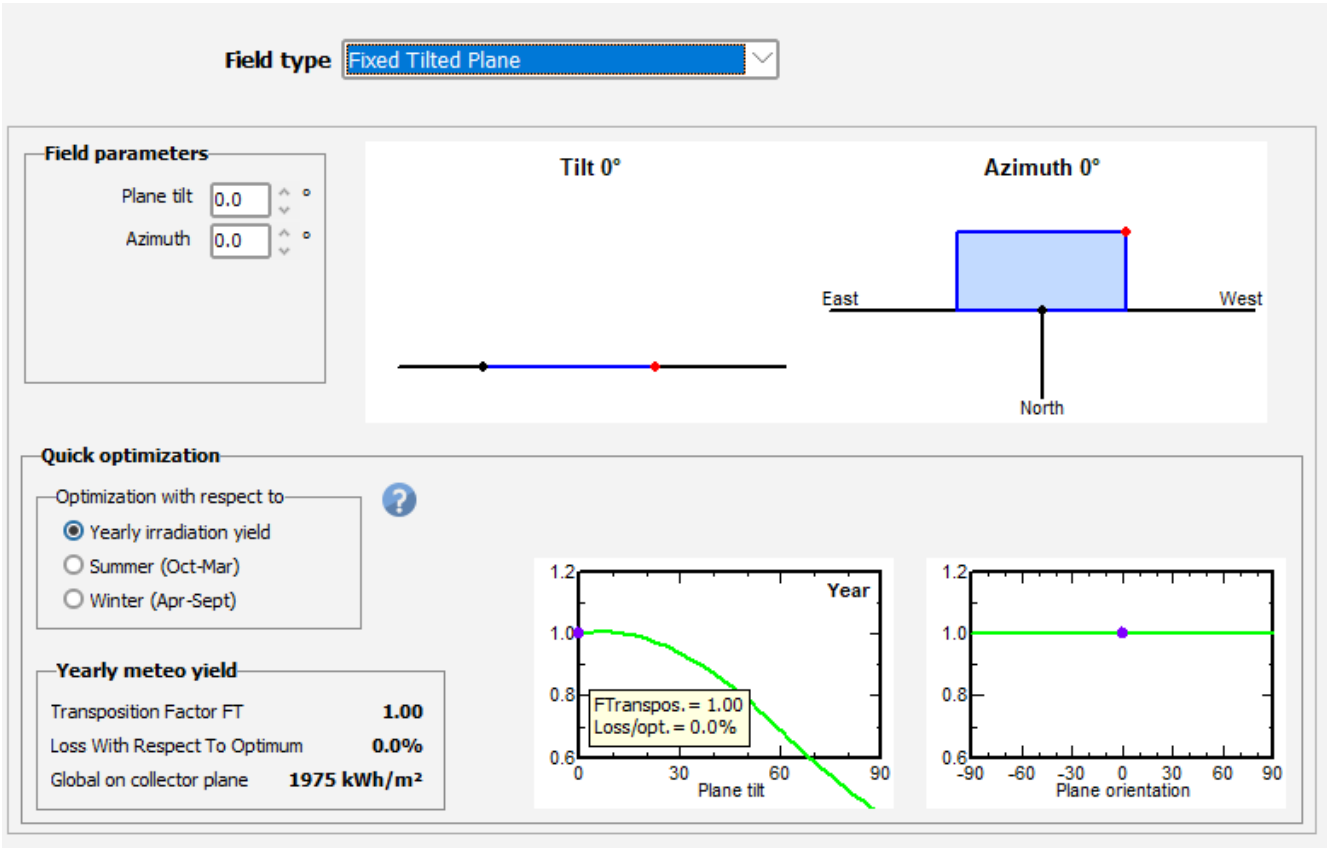

Appendix 8 : Panels orientation

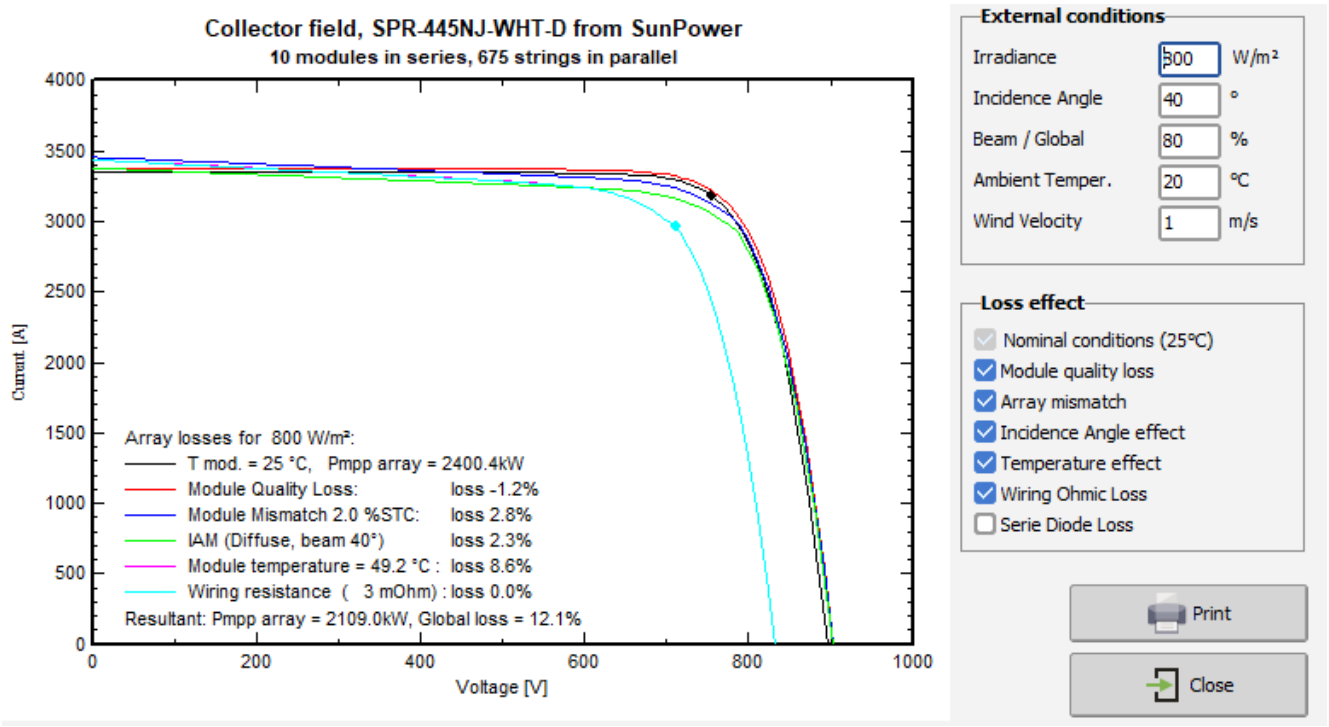

Appendix 9: PV array behavior for each loss effect

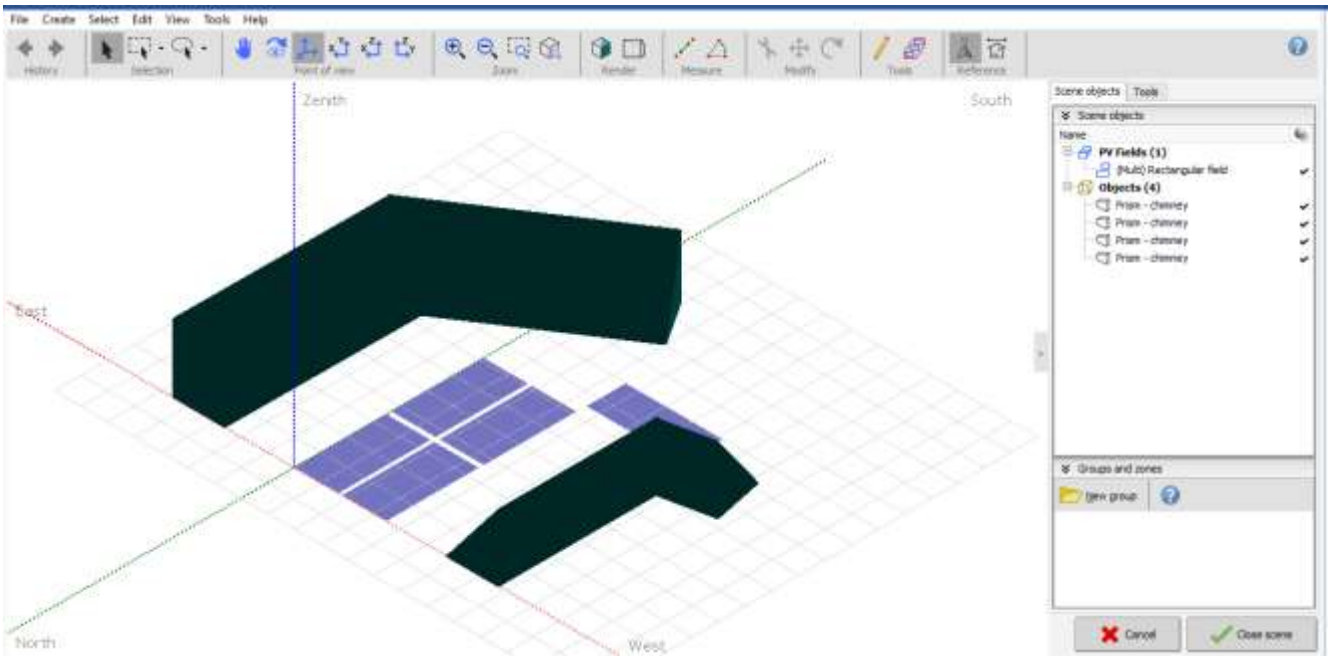

Appendix 10: Shading scene construction in PVsyst software